TOPICS IN QUARKONIUM PHYSICS*

By C. Quigg

Laboratoire de Physique Théorique, Ecole Normale Supérieure, Paris, France

and

Fermi National Accelerator Laboratory**, P.O. Box 500, Batavia, Illinois 60510, USA

(Received May 25, 1983)

The state of hadron spectroscopy in general and of heavy quark-antiquark bound states in particular is briefly reviewed. The first lecture is devoted to a summary of elementary techniques of quarkonium quantum mechanics. The second is concerned with inverse-scattering techniques. Throughout, the implications of recent data are assessed.

PACS numbers: 12.40.–y, 14.80.Dq

1. Why spectroscopy?

We live in the era of local gauge invariance, in which it appears that the fundamental interactions among the elementary constituents all may be derived from symmetry principles. This development has brought a greater unity to the interactions themselves and thus to particle physics, and has also brought our field into increased and fruitful contact with other specialties. The study of the early universe is one prominent example.

In spite of the structural appeal of gauge theories and the phenomenological successes of the Weinberg-Salam model and quantum chromodynamics, some central properties remain to be verified and many computational impediments remain to be overcome. Leaving aside the predicted properties of the intermediate bosons, we require a demonstration of the non-Abelian nature of the theories. In the case of the $SU(2)_L \otimes U(1)_Y$ electroweak theory, this is perhaps best done through the detailed study of radiative corrections to observable quantities. The existence of glueballs and the running of the strong coupling constant would provide relatively good evidence for the three-gluon interaction in QCD.

With respect to calculational difficulties, consider the comparison of perturbative QCD and experiment shown in Fig. 1. (This is a fabrication, but we have all heard similar

* Presented at the XXII Cracow School of Theoretical Physics, Zakopane, May 30–June 9, 1982.

** Permanent address; Fermilab is operated by Universities Research Association, Inc. under contract with the United States Department of Energy.

remarks in experimental seminars). Such a picture is sometimes shown with the comment that there is excellent agreement between perturbative QCD and experiment at 90°, and that elsewhere there is evidence for higher-twist effects. This is silly, of course, but higher--twist contributions or bound-state wavefunction effects are serious business. They are part of the reason that our comparisons between QCD and experiment are so unincisive.

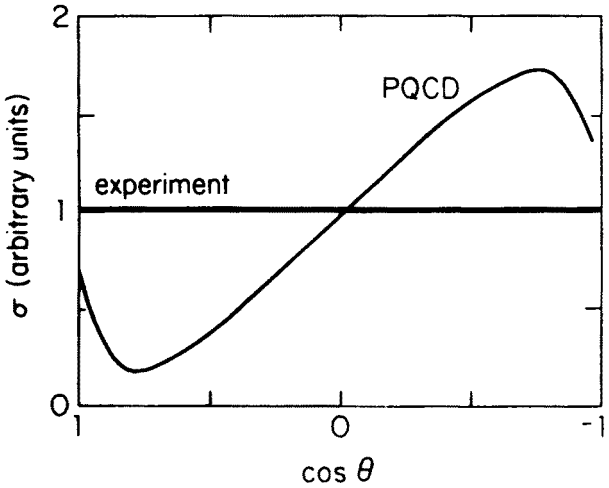

Fig. 1. Evidence for higher-twist effects?

The importance of spectroscopy can be dramatized in a different way by an appeal to pride. If you know the elementary particles (and we think we do, the quarks and leptons) and their interactions (we think we do, gauge theories) and you call yourself a physicist, you ought to be able to calculate the consequences. Although steady progress is being made in the investigation of lattice gauge theories, we have not yet learned to solve the strong interactions. Among our aspirations must be these:

— to compute the properties of hadrons, explain the absence of unseen species, and predict the existence of new varieties of hadrons;

— to explain why quarks and the quanta of the color interaction, gluons, are not observed in isolation.

— to derive the interactions among hadrons as a collective effect of the interactions among constituents.

For the moment these remain aspirations, but QCD does provide a framework in which to pursue such issues.

2. Bound states in QCD

It is widely held that QCD is a confining theory in the sense that only color-singlet objects can exist in isolation. An entirely rigorous demonstration has not yet been given for the continuum theory, but this belief is strongly supported by lattice calculations [1]. Granting that confinement occurs in QCD, we may ask how the theory would have to be

distorted to make it nonconfining. This line of inquiry is of importance both for the possibility that free quarks may someday be observed and for the insight it may provide into the nature of the confinement mechanism itself.

Although these deep issues remain incompletely resolved, QCD — as currently understood — has already provided insights or partial answers to many of spectroscopy's long-standing puzzles[1]. Among these are:

— the puzzle of triality, or the saturation of interquark forces;

— the equality (see Figs. 2 and 3) of the slopes of meson and baryon Regge trajectories;

— the chromomagnetic interaction, manifested in the fine structure and hyperfine structure of baryons, and in their decay systematics;

— the U(1) problem and other issues raised by current algebra — the successes of PCAC and the nature and consequences of chiral symmetry breaking;

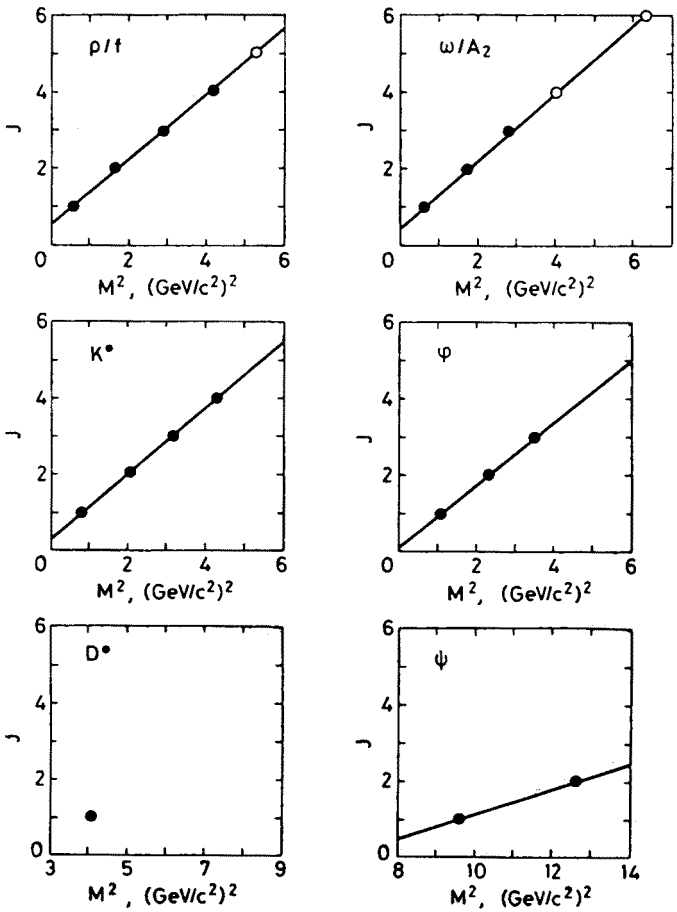

Fig. 2. Regge trajectories of the natural-parity mesons. Uncertain states are indicated by open circles

[1] Many of these points are treated more thoroughly in my 1981 Les Houches lectures, Ref. [2], where extensive and explicit references are given.

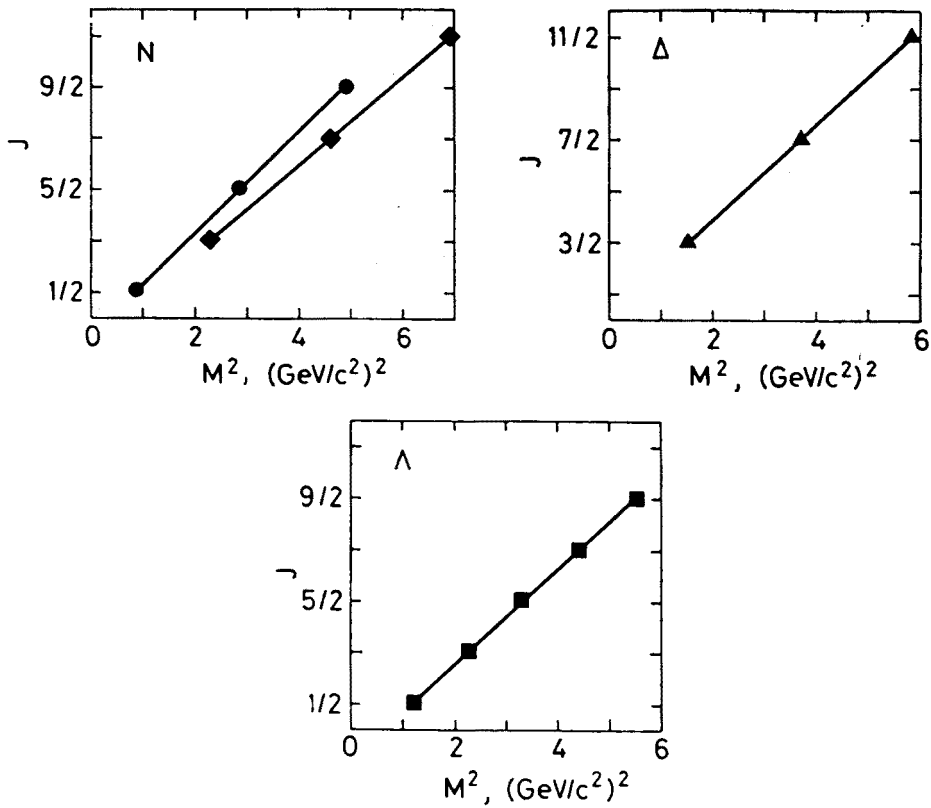

Fig. 3. Regge trajectories of the nucleon, Δ, and Λ baryon resonances

— the inhibitions of certain strong decays, as embodied in the Zweig rule, which arises naturally in the $SU(\to \infty)_{color}$ limit of QCD;[2]
— the nonrelativistic description of the quasiatomic bound states of quarks and antiquarks.
It is this last topic which is the focus of these lectures.

One of the basic issues on which we hope for enlightenment from QCD is this: why does the valence quark model work so well (but not perfectly?) Table I serves as a partial reminder that the elementary quark model is an admirable classification tool. In addition, the simple valence quark model provides useful insights into the electromagnetic structure of hadrons, as represented by the charge radii of the pseudoscalar mesons and of the neutron. The pattern of magnetic dipole transition rates in mesons is also anticipated by the model, and — with similar values for the quark dipole moments — a good account is given of the baryon magnetic dipole moments, as shown in Table II. Our experimental knowledge of these three classes of observables has been greatly improved by a series

[2] Why $SU(\infty)_c$ should so closely resemble $SU(3)_c$ remains to be clearly understood. This may eventually be a good lattice exercise.

TABLE I

Light Mesons as Quark-Antiquark Bound States

State	Mixing?	J^{PC}	$I = 1$	$I = 0$		$I = 1/2$
$^1S_0$		0^{-+}	$\pi(140)$	$\eta(549)$	$\eta'(958)$	K(496)
$^3S_1$	$^3D_1$	1^{--}	$\rho(776)$	$\omega(784)$	$\phi(1019)$	K*(892)
$^1P_1$		1^{+-}	B(1231)	H(1190)[a]		$Q_B(1355)$[b]
$^3P_0$		0^{++}	$\delta(981)$	$\epsilon(1300)?$[h]	S*(980)	$\varkappa(1500)?$?
$^3P_1$		1^{++}	$A_1(1240)$[a]	D(1285)	E(1418)	$Q_A(1340)$[b]
$^3P_2$	$^3F_2$	2^{++}	$A_2(1317)$	$f^0(1273)$	$f^*(1516)$	K**(1430)
$^1D_2$		2^{-+}	$A_3(1660)$			L(1765)?
$^3D_1$	$^3S_1$	1^{--}	$\rho'(1600)$		$\phi'(1634)$	K*(1650)?
$^3D_2$		2^{--}				
$^3D_3$	$^3G_3$	3^{--}	g(1700)	$\omega(1670)$	$\phi_3(1870)$[c]	K*(1753)[d]
$^1F_3$		3^{+-}				
$^3F_2$	$^3P_2$	2^{++}	$f\pi(1700)$[e]		$\theta(1640)$[g] ?	
$^3F_3$		3^{++}				
$^3F_4$		4^{++}	$K^+K_S(2060)$[f]	h(2040)		K*(2070)[d]

[a] J. A. Dankowych et al., *Phys. Rev. Lett.* **46**, 580 (1981).

[b] D. W. G. S. Leith, in *Experimental Meson Spectroscopy-1977*, edited by E. von Goeler and R. Weinstein, Northeastern University Press, Boston, p. 207.

[c] T. Armstrong et al., *Phys. Lett.* **110B**, 77 (1982).

[d] D. Aston et al., *Phys. Lett.* **106B**, 235 (1981). W. E. Cleland et al., *Phys. Lett.* **97B**, 465 (1980). P. A. Dorsaz, Université de Genève Thesis UGVA-Thèse-1994.

[e] R. J. Cashmore, in *Experimental Meson Spectroscopy-1980*, edited by S. U. Chung and S. J. Lindenbaum, American Institute of Physics, New York 1981, p. 1. L. Montanet, in *High Energy Physics--1980*, edited by L. Durand and L. G. Pondrom, American Institute of Physics, New York, p. 1196.

[f] W. E. Cleland et al., Université de Genève preprint UGVA-DPNC 1980/07-101. See also Montanet, op. cit.

[g] C. Edwards et al., *Phys. Rev. Lett.* **48**, 458 (1982).

[h] According to A. B. Wicklund et al., *Phys. Rev. Lett.* **45**, 1469 (1980), the pole lies at 1425 MeV.

of high-precision high-energy experiments. Further improvements are to be expected for the baryon magnetic moments, radiative transitions, and the closely related rate for two--photon decays of neutral mesons, the last from the study of $\gamma\gamma$ collisions in e^+e^- storage rings.

While the hadron spectrum has not been calculated from the basic field theory,[3] the quark model supplemented by dynamical assumptions inspired by QCD has led to increased understanding of the systematics. The order of levels and the signs and relative magnitudes of hyperfine splittings is well described by the picture exploited by De Rujula, Georgi, and Glashow [4]. Promising extensions to the orbitally-excited baryons have been made by Isgur and Karl and collaborators [5], although the dynamical basis of their *Ansatz* is questionable.

[3] There has been a good deal of progress toward *a priori* lattice QCD calculations of the spectrum. See the papers cited in Ref. [3].

TABLE II

Baryon Magnetic Moments (in nuclear magnetons)

Baryon	Quark Model	"Predictions"[a]	Experiment
p	$(4u-d)/3$	2.793	2.793
n	$(4d-u)/3$	−1.913	−1.913
Λ	s	−0.6138	-0.6138 ± 0.0047[b] -0.6129 ± 0.0045[c]
$\Lambda-\Sigma^0$	$(d-u)/\sqrt{3}$	−1.633	$-1.82^{+0.18}_{-0.25}$[d]
Σ^+	$(4u-s)/3$	2.673	2.33 ± 13[e] 2.357 ± 0.012[f] $2.368\pm0.014\pm0.04$[g]
Σ^0	$(2u+2d-s)/3$	0.791	
Σ^-	$(4d-s)/3$	−1.091	-1.41 ± 0.25 -1.151 ± 0.021[f] $-1.180\pm0.028\pm$??[g]
Ξ^0	$(4s-u)/3$	−1.436	-1.253 ± 0.014[f]
Ξ^-	$(4s-d)/3$	−0.494	-0.69 ± 0.04[f]

[a] Underlined values are inputs.

[b] L. Schachinger et al., *Phys. Rev. Lett.* **41**, 1348 (1978).

[c] P. T. Cox et al., *Phys. Rev. Lett.* **46**, 877 (1981).

[d] F. Dydak et al., *Nucl. Phys.* **B118**, 1 (1977).

[e] R. Settles et al., *Phys. Rev.* **D20**, 2154 (1979).

[f] L. G. Pondrom, contribution to the 5th International Symposium on High Energy Spin Physics, Brookhaven 1982.

[g] J. P. Marriner et al., FERMILAB-Conf-82/85-EXP, contribution to the 5th International Symposium on High Energy Spin Physics, Brookhaven 1982.

TABLE III

Candidates for Radially-Excited Pseudoscalars

State	Isospin	Seen In	Reference
$\pi'(1342)$	1	$\varepsilon\pi$	M. Bonesini et al., *Phys. Lett.* **103B**, 75 (1981).
$\eta(1275)$	0	$\eta\pi\pi$	N. Stanton et al., *Phys. Rev. Lett.* **42**, 346 (1981).
$\eta'(1400)$	0	$\eta\varepsilon$	Stanton et al., quoted by F. E. Close, Ref. [5].
$\iota(1440)$	0	$\psi\to\gamma+(K\bar{K}\pi)$	C. Edwards et al., *Phys. Rev. Lett.* **49**, 259 (1982); D. L. Scharre et al., *Phys. Lett.* **97B**, 329 (1980).
$K'(1400)$	$\frac{1}{2}$	$K\pi\pi(K\varepsilon)$	G. Brandenburg et al., *Phys. Rev. Lett.* **36**, 1239 (1976); D. Aston et al., *Phys. Lett.* **106B**, 235 (1981).

The phenomenology of *radially*-excited states is less developed. Among the mesons composed of light quarks, only a handful of candidates for radial excitations are known. It is likely that the vector mesons $\varrho'(1600)$ and $\phi'(1634)$ are, or are considerably mixed with, 2^3S_1 radial excitations of the familiar vector mesons. Increasing attention is being devoted to the study of pseudoscalar states beyond the familiar nonet [6]. Some of these are collected in Table III. If these are indeed $(q\bar{q})$ states, they are necessarily radial excitations, because the quantum numbers $J^{PC} = 0^{-+}$ do not occur in orbitally-excited states. Other interpretations of new pseudoscalar levels as glueballs or multiquark states are tenable only if the $(q\bar{q})$ interpretation can be ruled out. This is therefore an issue of more than passing importance. In the heavy-quark families ψ and Υ, essentially pure radial excitations are commonplace, as we shall discuss below.

3. Beyond the quark model

To the extent that we gain an understanding of the dynamics of strong interactions, we may reasonably hope to advance beyond the simple quark model rules. In so doing, we open to discussion states which are described only symbolically — or not at all — by the elementary scheme. Multiquark states and hadrons which manifest the gluonic degrees of freedom may be considered in this broader context.

Multiquark hadrons include $(qq\bar{q}\bar{q})$ exotic mesons, $(4q\bar{q})$ exotic baryons, and stable (6q) dibaryons. Although color-singlet multiquark configurations are readily constructed, elementary color-saturation arguments give no reason to expect that they should be strongly bound. However, as Jaffe [7] has emphasized, in special circumstances the color hyperfine interaction might be strong enough to provide the binding force. On the basis of this reasoning, he has conjectured a lightly-bound $\Lambda\Lambda$ bound state. A first experimental search [8] was unsuccessful. Similar considerations [9] have been applied to $(qq\bar{q}\bar{q})$ "baryonium" states for which there is at the moment no experimental evidence.

In the second category lie hybrid states such as $(q\bar{q}g)$ or (qqqg) [11], "vibrational modes" of heavy $Q\bar{Q}$ systems [12], and quarkless states known variously as gluonia, gluonic mesons, or glueballs [13]. Establishment of hadrons composed exclusively of gluons would constitute strong evidence in favor of the correctness of QCD, and would specifically test the existence of the nonlinear gluon interactions.

Over the past few years, an interesting candidate has come forward: the $J^{PC} = 0^{-+}$ $\iota(1440)$, seen in the decay

$$\psi \to \gamma(K\bar{K}\pi). \tag{3.1}$$

Some of the evidence [14] for this state is shown in Fig. 4. The correlation between the prominence of the signal and the low-$K\bar{K}$-mass cut is suggestive of the decay chain

$$\begin{array}{l} \iota \to \delta(980)\pi \\ \qquad \big\lfloor\!\!\longrightarrow K\bar{K}. \end{array} \tag{3.2}$$

This idea is supported, though not established, by the Dalitz plot distribution given in Fig. 5, which does not show prominent K* bands. The verdict is not clearcut because of

the limited phase space available for the decay, and the fact that the K* bands would overlap in the δ region. (I show the Dalitz plot here, however, not to enter into the details of iotology but to remark on its sparseness, in an analysis based on 2.2×10^6 ψ triggers. It is frustrating that a significant increase in statistics is unlikely to materialize). The interest in this state derives in no small part from the relatively large branching ratio for the decay $\psi \to \gamma\iota(1440)$, which suggests a connection with

$$\psi \to \gamma gg, \tag{3.3}$$

with

$$J^{PC}(gg) = 0^{++}, 0^{-+}, 2^{++}, \text{ etc.}$$

Two important theoretical questions arise at once: what is the mass scale for glueballs and how prominently will they appear in the spectrum of hadrons? Given the small mass of the pion it is nearly a certainty that the lightest glue state will be unstable. We must then ask whether the quarkless states will become so broad as to be lost in a general continuum, whether they will mix so strongly with $(q\bar{q})$ and $(q\bar{q}g)$ states as to lose their identity, or whether they will remain relatively pure glue states of modest width. Distinguishing gluonia from ordinary $(q\bar{q})$ states will require a detailed knowledge of meson spectroscopy. One simple example of the kind of studies that may be undertaken is the

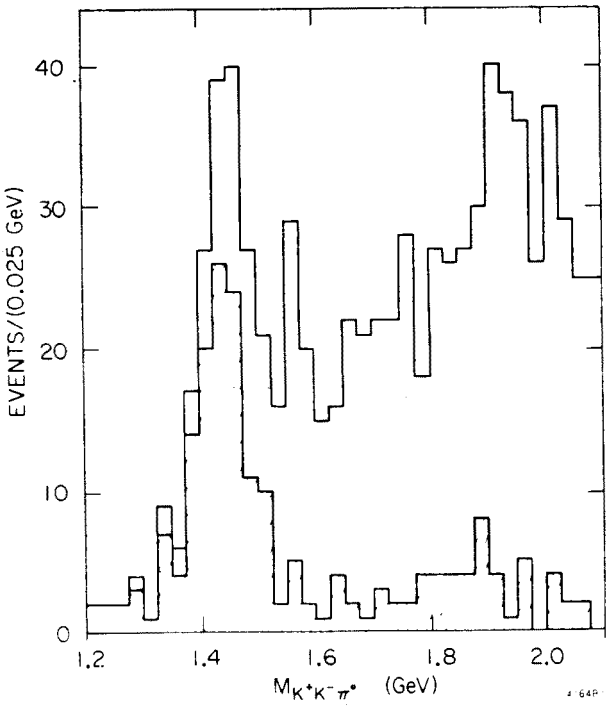

Fig. 4. $K^+K^-\pi^0$ invariant mass distribution for events consistent with the hypothesis $\psi \to \gamma(K^+K^-\pi^0)$. Shaded histogram has the requirement $M(K\bar{K}) < 1125$ MeV/c^2. (From Ref. [14])

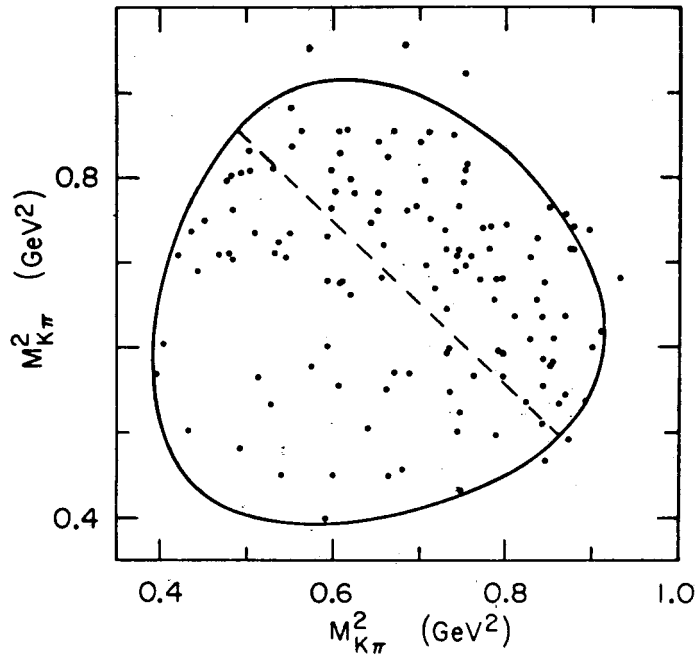

Fig. 5. $K^+K^-\pi^0$ Dalitz plot for events with 1400 MeV/$c^2 \leqslant M(K^+K^-\pi^0) \leqslant$ 1500 MeV/c^2. Solid curve shows the boundary for $M(K\bar{K}\pi) = 1450$ MeV/c^2. The dashed line indicates $M(K\bar{K}) = 1125$ MeV/c^2. (From Ref. [14])

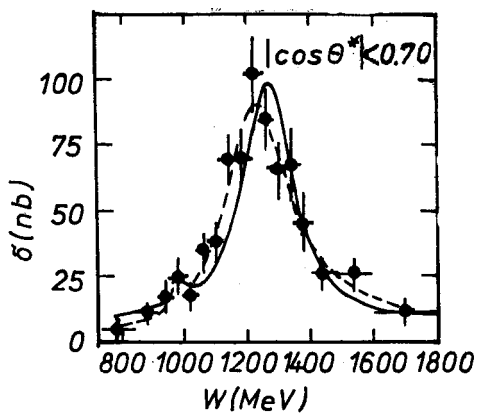

Fig. 6. Cross section for $\gamma\gamma \to \pi^0\pi^0$ (for $|\cos\theta^*| < 0.7$), as a function of the $\pi^0\pi^0$ invariant mass W. θ^* is the angle between the beam direction and a π^0 measured in the $\pi^0\pi^0$ rest system. (From Ref. [15])

comparison of bosons produced in radiative quarkonium decays (3.3), which should emphasize gluonic constituents, with those produced in two-photon collisions

$$\gamma\gamma \to q\bar{q}, \tag{3.4}$$

which should emphasize quark constituents. The similarities and differences should illuminate the nature of the possibly mixed mesons concerned.

A provocative observation is the line shape of the $f^0(1273)$ observed [15] in the two-photon process

$$\gamma\gamma \to f^0 \to \pi^0\pi^0, \tag{3.5}$$

shown in Fig. 6, which is shifted downward by approximately 40 MeV/c^2 compared with the standard f^0 detected in hadronic collisions and in [16] $\psi \to \gamma f^0$.

4. Why quarkonium?

After this brief tour of spectroscopy in general, which was intended to place the subject in the broader context of elementary particle physics, and to evoke its importance for the evolution of QCD, we turn now to a discussion of the heavy mesons known as quarkonium. These are not merely of typical spectroscopic interest, but also have special features which attract our attention. Because of asymptotic freedom, they may provide us with another access [17] to perturbative QCD. This has two important operational consequences: The utility of nonrelativistic methods, and the goodness of the valence quark model approximation as a perturbative statement, in addition to the familiar encouragements of experience and the $1/N$ expansion.

In the ψ and Υ families, we are approaching for the first time a truly predictive spectroscopy, and also have the opportunity to probe the strong interaction between quarks in new ways. We have been able to "measure" the form of the $Q\overline{Q}$ interaction at intermediate (0.1 fm $< r <$ 1 fm) distances. Many methods are by now available, so there is a good measure of control over the systematic uncertainties of these determinations. Quarkonium also offers the advantage of a large, and growing, body of beautiful data, which presents us with many things to understand and opens the opportunity for a creative interplay between theory and experiment. Knowledge of the interquark potential is also of interest for what may be called "engineering" purposes: comparing expectation with observation for quarkonia is a superb tool for probing the flavor and color properties of new quarks.

What expectations for the interquark interactions should we have before looking at any data? According to the conventional wisdom, at small distances the potential should approach the Coulomb form

$$V(r) \sim -4\alpha_s/3r \tag{4.1}$$

characteristic of the exchange of a single massless gluon. At large distances, a popular conjecture is that the potential (to the extent that it has meaning) approaches a linear form

$$V(r) \sim r/a^2 \tag{4.2}$$

contrived to confine the quarks. Between these limits of perturbative QCD calculation and Reggeistic inspiration we are ignorant of the force law. The simplest guess [18] is that the potential takes the form

$$V(r) = -4\alpha_s/3r + r/a^2. \tag{4.3}$$

The quark mass m_q, the strong coupling constant α_s, and the string tension $1/a^2$ are then taken as parameters which may be adjusted to reproduce features of the observed spectrum.

Although the simple form provides an extremely useful first guess, we shall find that the distance scale to which observables are sensitive is precisely that intermediate region in which we are ignorant. It also develops that observables are rather insensitive to assumptions about large- and small-r behavior. It is therefore in our interest to discuss ways of determining the interaction which are free from $r \to 0$ and $r \to \infty$ prejudices.

5. *The spin-singlet states of charmonium*

Important progress has been made recently in identifying the $^1S_0$ hyperfine partners of the $^3S_1\psi$ and ψ' levels of charmonium. The particle known as U(2.98) is now securely established [19] as the $\eta_c(2983 \pm 5)$, with a total width of 12 ± 4 MeV. The hyperfine splitting,

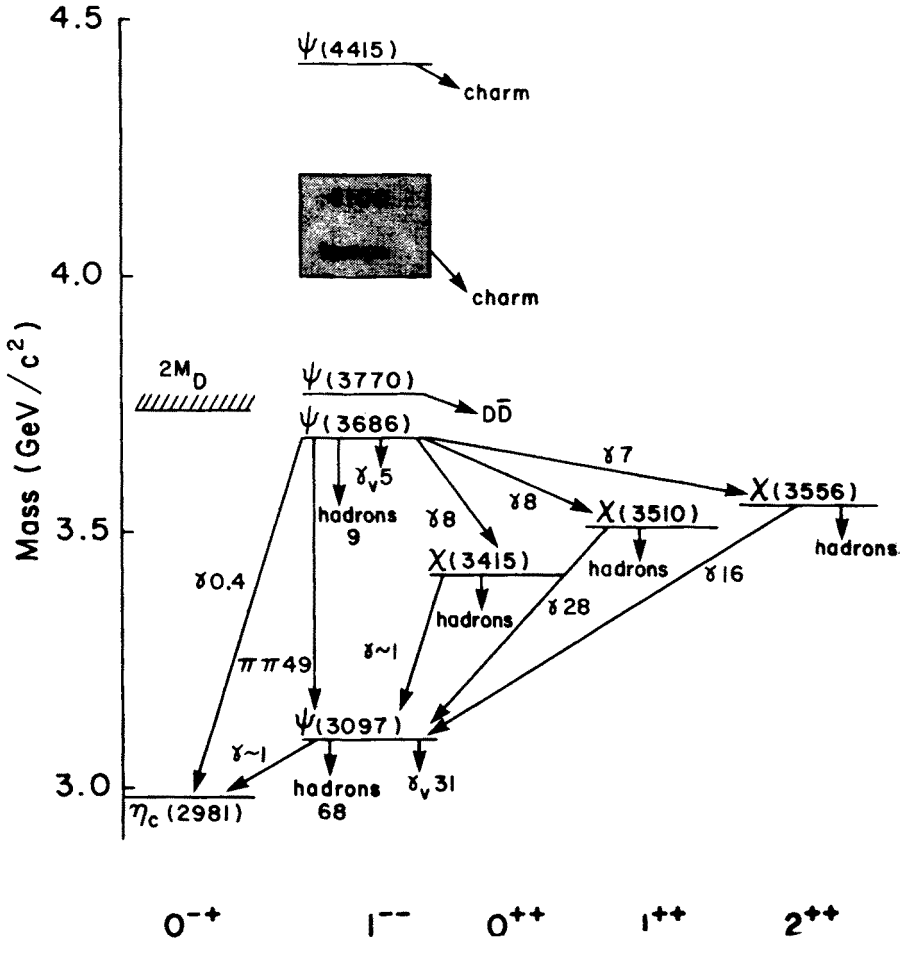

Fig. 7. The spectrum of charmonium

$M(\psi)-M(\eta_c) = 114\pm5$ MeV/c^2, is in reasonable accord with theoretical expectations. The η_c has been seen in the $M1$ transitions $\psi \to \gamma\eta_c$, $\psi' \to \gamma\eta_c$, at rates given by

$$\Gamma(\psi \to \gamma\eta_c)/\Gamma(\psi \to \text{all}) = (1.20^{+0.36}_{-0.31})\%, \tag{5.1}$$

which implies

$$\Gamma(\psi \to \gamma\eta_c) = 0.44-0.95 \text{ keV}; \tag{5.2}$$

and

$$\Gamma(\psi' \to \gamma\eta_c)/\Gamma(\psi \to \text{all}) = (0.32\pm0.05\pm0.05)\%, \tag{5.3}$$

which implies

$$\Gamma(\psi' \to \gamma\eta_c) = (0.69\pm0.23\pm0.11) \text{ keV}. \tag{5.4}$$

The 2^1S_0 radial excitation $n_c'(3592\pm5)$, with a total width less than 9 MeV, has been observed [20] in the transition $\psi' \to \gamma\eta_c'$, with

$$\Gamma(\psi' \to \gamma\eta_c')/\Gamma(\psi' \to \text{all}) = (0.6\times2^{\pm1})\%, \tag{5.5}$$

which implies

$$\Gamma(\psi' \to \gamma\eta_c') = (1.3\times2^{\pm1}) \text{ keV}. \tag{5.6}$$

The hyperfine interval, $M(\psi')-M(\eta_c') = 92\pm5$ MeV/c^2, is of approximately the expected magnitude.

With these additions, the spectrum of psions is as shown in Fig. 7. Among the expected narrow levels, only the 2^1P_1 state remains to be observed. Its mass is expected to coincide with the centroid of the ^3P_J masses, at about 3525 MeV/c^2.

6. Upsilon update

The principal experimental progress in recent months has been in establishing an absolute scale for the Υ mass and in finding the first evidence for electromagnetic transitions to orbitally excited states. In addition, mass splittings and leptonic widths have been refined somewhat.

A precision measurement of the Υ mass was carried out at Novosibirsk using the resonance depolarization method to provide an absolute calibration of the machine energy. The result is [21]

$$M(\Upsilon) = (9459.7\pm0.6) \text{ MeV}/c^2. \tag{6.1}$$

Current knowledge of the basic properties of the $^3S_1$ vector states is summarized in Table IV.

The first studies of the $E1$ transitions between S and P states have been carried out by the CUSB Collaboration working at CESR. They have observed the $3^3S_1 \to \gamma+2^3P_J$ radiation, and have determined [22] the center of gravity of the 2^3P_J levels as 10.255 ± 0.004 GeV/c^2. Current knowledge of the upsilons[4] is summarized in Fig. 8.

[4] The $B\bar{B}$ threshold is based on Ref. [23].

TABLE IV

Properties of the $^3S_1$ Upsilon Levels

	Υ	Υ'	Υ''	Υ'''
Mass (MeV/c^2)	9459.7±0.6[a]	10019.1	10350.3	10572.4
$M-M(\Upsilon)$ (MeV/c^2)	—	559.4±2.5	890.6±0.5[b]	1112.7±4.1
Γ_{ee}(keV)	1.15±0.13	0.54±0.03	0.35±0.03	0.25±0.06
Γ_{total}(keV)	42.2±14.9	$=\Gamma(\Upsilon)$	$=\Gamma(\Upsilon)$	14.4±5.2 MeV

[a] A. S. Artamonov et al., *Phys. Lett.* **118B**, 225 (1982).
[b] P. Franzini, J. Lee-Franzini, *Phys. Rep.* **81**, 239 (1982).

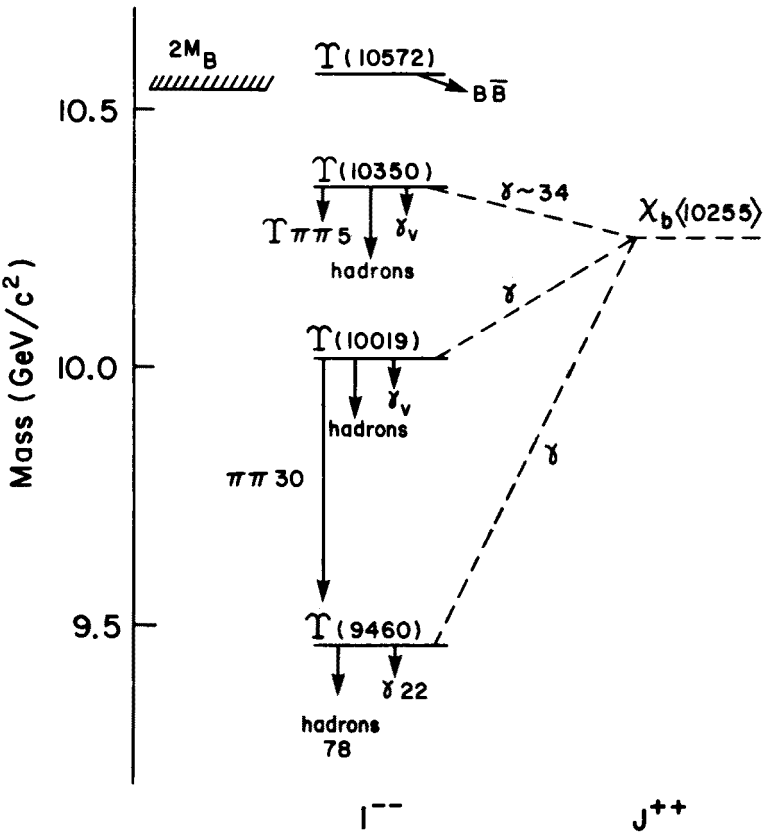

Fig. 8. The upsilon spectrum

In the near future, we may look forward to a steady flow of new results from CESR. In addition, the new ARGUS detector and the transplanted Crystal Ball are coming into operation at the rebuilt DORIS II machine in Hamburg. Thus we may reasonably expect much new information about the upsilon spectrum over the next few years.

7. Scaling the Schrödinger equation

For simple potentials, including power-laws and other monotonic wells, rather far-reaching results can be derived using quite elementary techniques. This mode of analysis has been reviewed by Quigg ynd Rosner [24], and exploited by many authors. I shall summarize here a few of the results with direct applications to experiment.

7.1. Dependence on constituent mass and coupling constant

The reduced radial Schrödinger equation for a particle with mass μ and angular momentum l moving in a central potential V may be written in the form

$$\frac{\hbar^2}{2\mu}u''(r)+\left[E-V(r)-\frac{l(l+1)\hbar^2}{2\mu r^2}\right]u(r)=0, \tag{7.1}$$

subject to the boundary conditions

$$u(0)=0, \qquad u'(0)=R(0). \tag{7.2}$$

A prime is used to denote derivatives with respect to the argument, and the reduced radial wavefunction $u(r)$ is related to the three-dimensional wavefunction

$$\Psi(r)=R(r)Y_{lm}(\theta,\phi) \tag{7.3}$$

by

$$u(r)=rR(r). \tag{7.4}$$

The familiar substitution (7.4) places the radial equation in three dimensions in formal correspondence with the one-dimensional Schrödinger equation.

For the special case of a power-law potential,

$$V(r)=\lambda r^{\nu}, \tag{7.5}$$

the equation (7.1) can be divested of all its dimensionful parameters. To see this, we first introduce a scaled measure of length

$$\varrho \equiv (\hbar^2/2\mu|\lambda|)^p r, \tag{7.6}$$

where the exponent p is to be chosen to eliminate dimensions from (7.1). The choice

$$p=-1/(2+\nu), \tag{7.7}$$

when accompanied by the substitutions

$$E=\left(\frac{\hbar^2}{2\mu}\right)\left(\frac{\hbar^2}{2\mu|\lambda|}\right)^{2p}\varepsilon, \tag{7.8}$$

where ε is dimensionless, and

$$w(\varrho)=u(r) \tag{7.9}$$

accomplishes precisely this. The ensuing equation is

$$w''(\varrho)+[\varepsilon-\mathrm{sgn}\,(\lambda)\varrho^{\nu}-l(l+1)/\varrho^2]w(\varrho)=0, \tag{7.10}$$

which depends only upon pure numbers.

Several consequences follow immediately from these manipulations. Lengths and quantities with the dimensions of lengths depend upon the constituent mass and coupling strength as

$$L \propto (\mu|\lambda|)^{-1/(2+\nu)}. \tag{7.11}$$

As a result, the particle density at the origin of coordinates behaves as

$$|\Psi(0)|^2 \sim L^{-3} \propto (\mu|\lambda|)^{3/(2+\nu)}. \tag{7.12}$$

Level spacings have a similarly definite behavior, according to (7.8):

$$\Delta E \propto \mu^{-\nu/(2+\nu)}\ |\lambda|^{2/(2+\nu)}. \tag{7.13}$$

The limiting behavior of the scaled Schrödinger equation as $\nu \to 0$ is easily studied. The "power-law" potential corresponding to this limit is simply

$$V(r) = C\log(r). \tag{7.14}$$

The scaling laws (7.11)–(7.13) contain many well-known results. Recall, for example, that in the Coulomb potential, for which $\nu = -1$,

$$\Delta E(\nu=-1) \propto \mu\alpha^2 = \mu|\lambda|^2. \tag{7.15}$$

Likewise, the conclusion that in a linear potential

$$|\Psi(0)|^2|_{\nu=1} \propto \mu|\lambda| \tag{7.16}$$

can be derived at once using the identity

$$|\Psi(0)|^2 = \frac{\mu}{2\pi\hbar^2}\left\langle\frac{dV}{dr}\right\rangle. \tag{7.17}$$

The scaling laws (7.11)–(7.13) have many applications in quarkonium physics. For the moment let us merely note that electric multipole matrix elements vary as

$$\langle n'|Ej|n\rangle \sim L^j \propto (\mu|\lambda|)^{-j/(2+\nu)}, \tag{7.18}$$

so that transition rates behave as

$$\Gamma(Ej) \sim k^{2j+1}|\langle n'|Ej|n\rangle|^2, \tag{7.19}$$

where k is the energy of the radiated photon, which is just a level spacing ΔE. Using (7.11) and (7.13) we then deduce that

$$\Gamma(Ej) \propto \mu^{-[2j(1+\nu)+\nu]/(2+\nu)}|\lambda|^{2(j+1)/(2+\nu)}. \tag{7.20}$$

This has the interesting consequence that for fixed potential strength $|\lambda|$, $\Gamma(Ej)$ is a decreasing function of j as $\mu \to \infty$ for potentials less singular than the Coulomb potential.

Using the Van Royen-Weiskopf formula [25]

$$\Gamma(V^0 \to e^+e^-) = \frac{16\pi\alpha^2}{M_V^2} |\Psi(0)|^2 \langle e_q^2 \rangle \tag{7.21}$$

for vector meson decay, one may easily show that for $\nu > -1$ (for which binding energies are asymptotically negligible)

$$\Gamma(Ej)/\Gamma(V^0 \to e^+e^-) \propto \mu^{-(2j-1)(\nu+1)/(2+\nu)} |\lambda|^{2(j-1)/(2+\nu)}, \tag{7.22}$$

which implies the dominance of leptonic over radiative decays as $\mu \to \infty$ for fixed potential strength $|\lambda|$.

7.2. Dependence on principal quantum number

To investigate how observables depend upon the principal quantum number with some degree of generality it is convenient to adopt the semiclassical, or JWKB approximation. This turns out to be rather less of a compromise than one might at first surmise. Judiciously applied, the semiclassical approximation is in fact highly accurate for the sort of nonpathological potentials one hopes to encounter for quarkonium. This accuracy is documented in Ref. [24], where additional references may be found.

The semiclassical results all follow from the quantization condition

$$\int_0^{r_c} dr[2\mu(E - V(r))]^{1/2} = (n - \tfrac{1}{4})\pi\hbar, \tag{7.23}$$

where n is the principal quantum number and the classical turning point r_c is defined through $V(r_c) = E$. Although it is both possible and useful to be more general, it is appropriate to retain the spirit of the preceding Section and specialize to power-law potentials. For s-wave bound states of nonsingular potentials of the form (7.5), Eq. (7.23) can be integrated by elementary means to yield

$$E_n \propto (n - \tfrac{1}{4})^{2\nu/(2+\nu)} \tag{7.24}$$

where with an eye toward the intended applications I have suppressed the dependence on constituent mass and coupling strength given in (7.13). For singular potentials additional care is required near the origin. A simple modification of the usual procedure leads to

$$E_n \propto (n - \gamma(\nu))^{2\nu/(2+\nu)}, \qquad -2 < \nu < 0, \tag{7.25}$$

where

$$\gamma(\nu) = \tfrac{1}{2}\left(\frac{1+\nu}{2+\nu}\right). \tag{7.26}$$

Similar expressions may be obtained for orbitally-excited states.

By evaluating the expectation value in Eq. (7.17) with JKWB wavefunctions, it is also straightforward to derive

$$|\Psi_n(0)|^2 \propto \begin{cases} (n-\frac{1}{4})^{2(\nu-1)/(2+\nu)}, & \nu > 0, \quad (7.27a) \\ (n-\gamma(\nu))^{(\nu-2)/(2+\nu)}, & 0 > \nu > -2. \quad (7.27b) \end{cases}$$

For a *general* nonsingular potential, one may readily show that

$$|\Psi_n(0)|^2 = \frac{(2\mu E_n)^{1/2}}{4\pi^2\hbar^3} \frac{\partial(2\mu E_n)}{\partial n}. \quad (7.28)$$

Generalizations of these results to $l \neq 0$ have also been made, but we shall not require them here. Let us now see what can be learned by comparing the simple results of this Section with experimental information.

8. *Inferences*

The strategy embodied in Sec. 7 has been pursued explicitly by several authors [24, 26–29] and implicitly by many others. The conclusion to be drawn from the data is that a potential of the form

$$V(r) = A + Br^{\nu} \quad (8.1)$$

with $\nu = 0.1$ gives a good representation of the ψ and Υ spectra. This is based upon four distinct kinds of evidence.

First, we may note by comparing Figs. 7 and 8 that the level spacings are quite similar in the ψ and Υ families. Indeed, the observation that

$$M_{\Upsilon'} - M_{\Upsilon} = M_{\psi'} - M_{\psi} \quad (8.2)$$

provided an early motivation for the logarithmic potential [27]. A more detailed look

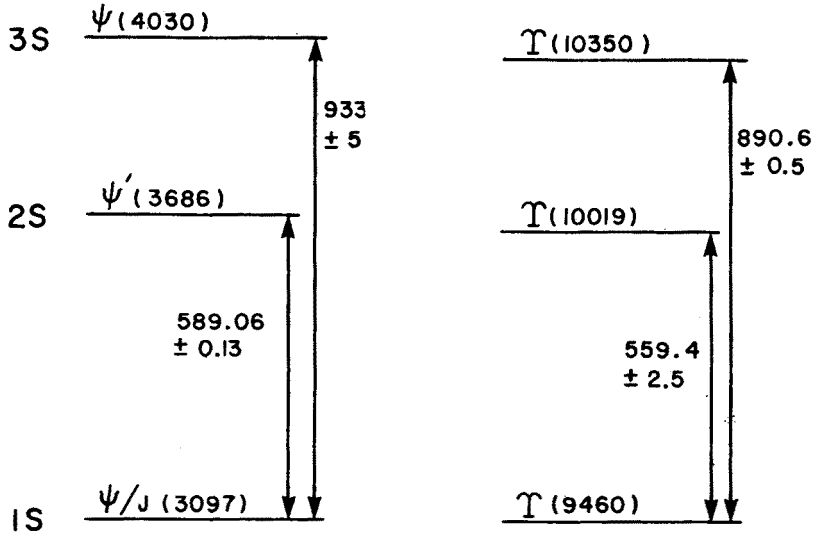

Fig. 9. Level spacings in the ψ and Υ families

at the intervals is given by Fig. 9, which indicates that

$$\Delta E(\Upsilon) - 0.95\,\Delta E(\psi). \tag{8.3}$$

Assuming that the potential strength does not vary between the ψ and Υ systems, this implies a small positive power for the effective potential. The precise value of the exponent depends upon the ratio of quark masses, which is imperfectly known.

The principal-quantum-number dependence of observables within one quarkonium system is free from the assumption that the potential strength λ is the same for different quark flavors. Effective powers may be inferred independently from the ψ and Υ levels and compared for consistency. The level structures $(E_3-E_2)/(E_2-E_1)$, etc. are characteristic of the potential shape. These ratios of intervals are the same for ψ

$$\left.\frac{E_3-E_2}{E_2-E_1}\right|_{\psi} = 0.58$$

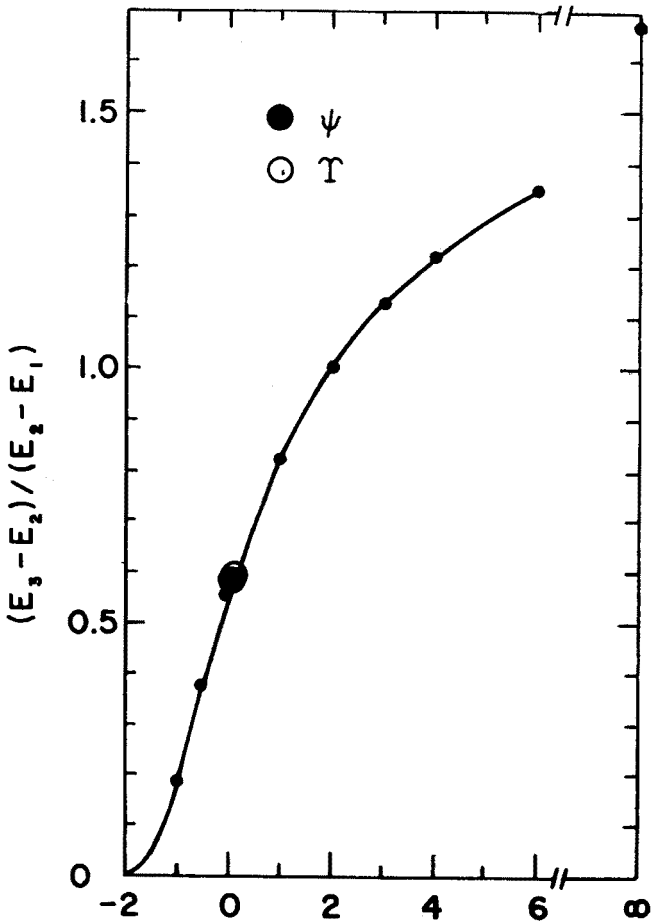

Fig. 10. Semiclassical (curve) and exact (small dots) ratios $(E_3-E_2)/(E_2-E_1)$ for s-wave levels in potentials $V(r) = \lambda r^{\nu}$. (From Ref. [24])

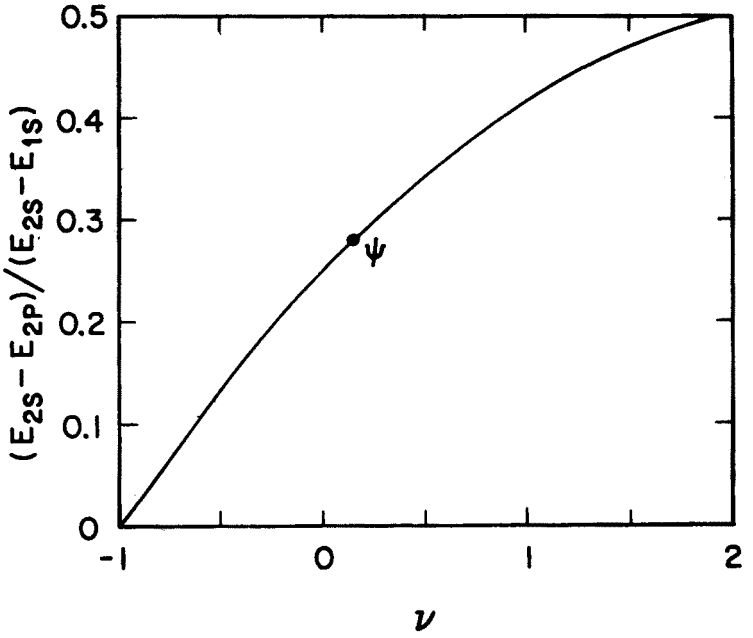

Fig. 11. The quantity $(E_{2S}-E_{2P})/(E_{2S}-E_{1S})$ for power-law potentials $V(r)=\lambda r^{\nu}$, $-1<\nu<2$. The datum is the value in the charmonium system

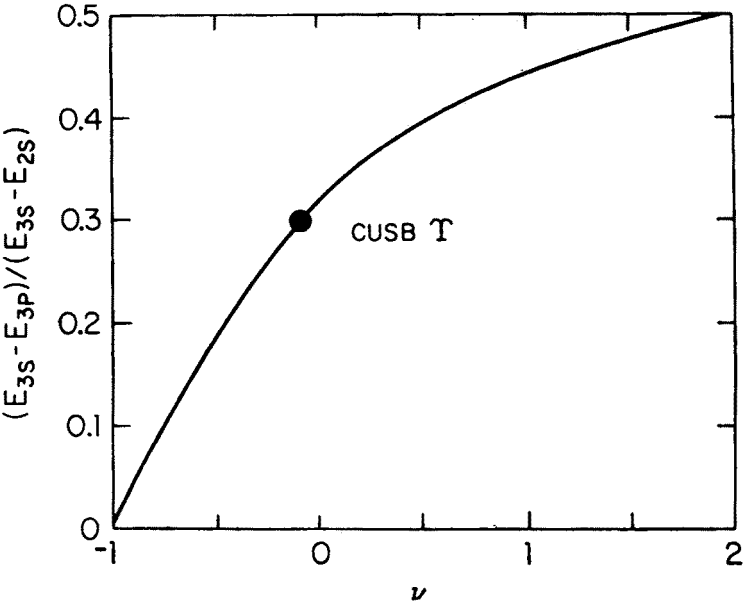

Fig. 12. The quantity $(E_{3S}-E_{3P})/(E_{3S}-E_{2S})$ for power-law potentials $V(r)=\lambda r^{\nu}$, $-1<\nu<2$ (C. Quigg and J. L. Rosner, unpublished). The datum is based on the CUSB observation, Ref. [22]

and Υ

$$\left.\frac{E_3-E_2}{E_2-E_1}\right|_{\Upsilon} = 0.59 \tag{8.4}$$

states, and are again compatible with $\nu = 0.1$, as shown in Fig. 10. Similarly, the $2S-2P$ spacing, known only for the ψ family (Fig. 11), implies a small positive power. The $3S-3P$ interval in the upsilon system is also characteristic of a power near zero, but slightly negative as shown in Fig. 12. The same is true of the ratio $(E_4-E_3)/(E_3-E_2)$ in the Υ family, displayed in Fig. 13. Finally, the principal quantum number dependence of wavefunctions at the origin, or equivalently of the reduced leptonic widths

$$\tilde{\Gamma}(V^0 \to e^+e^-) \equiv M_V^2\Gamma(V^0 \to e^+e^-), \tag{8.5}$$

is approximately given by

$$|\Psi_n(0)|^2 \sim 1/(n-\tfrac{1}{4}) \tag{8.6}$$

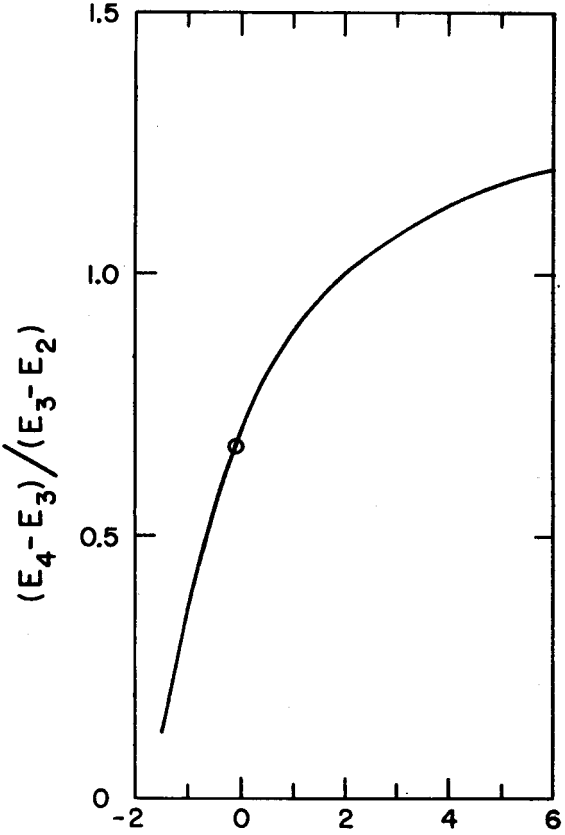

Fig. 13. The quantity $(E_4-E_3)/(E_3-E_2)$ for s-wave levels in power-law potentials $V(r) = \lambda r^\nu$, $-1 \leqslant \nu \leqslant 2$. The datum is the value in the upsilon system

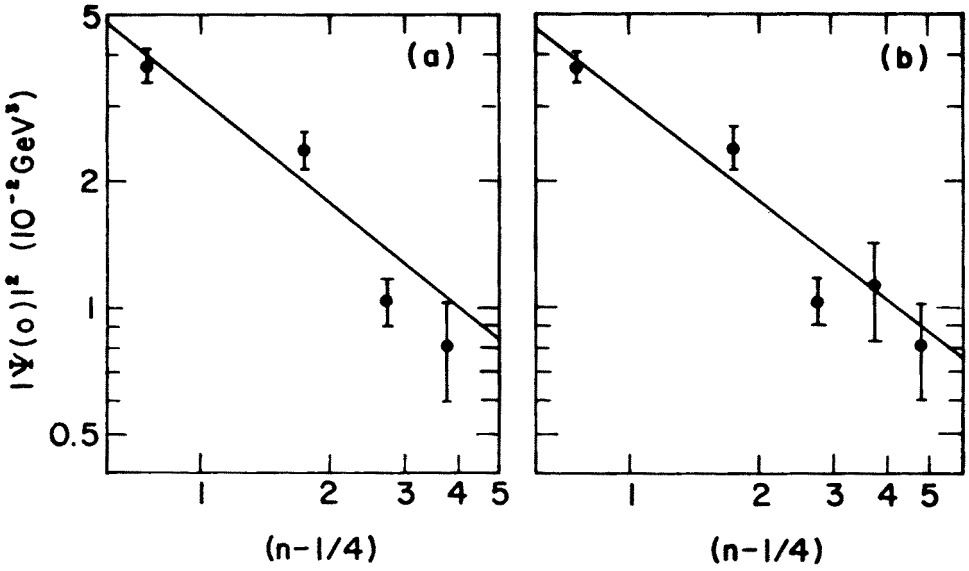

Fig. 14. Square of the wavefunction at the origin of the psions. Possible mixing between the $2^3S_1(3686)$ and $3^3D_1(3770)$ levels has been neglected. (a) A best fit proportional to $(n-1/4)^p$, with $p = -0.83 \pm 0.11$ ($\nu = 0.12 \pm 0.08$), assuming the conventional $4S$ assignment for $\psi(4415)$. (b) An alternative $5S$ assignment for $\psi(4415)$, which corresponds to $p = -0.79 \pm 0.10$ ($\nu = 0.15 \pm 0.08$). In plotting the data against $(n-1/4)$, we have anticipated the result $p > -1$ ($\nu > 0$)

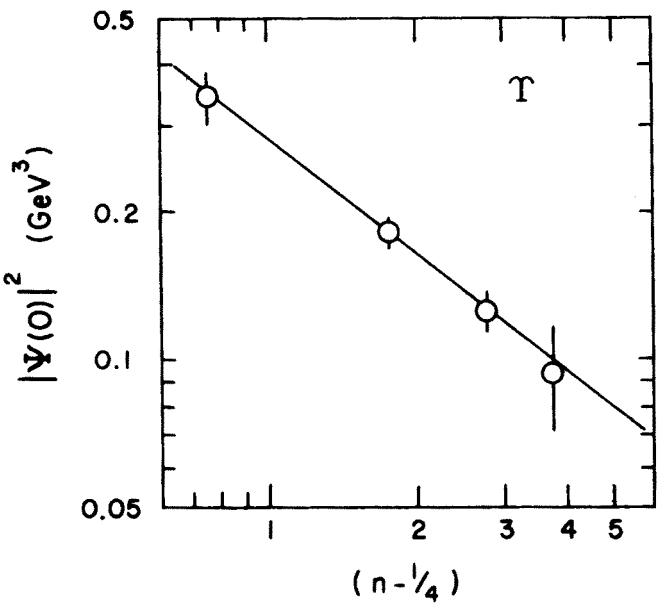

Fig. 15. Same as Fig. 14 for the upsilons. The best fit is for $p = -0.79 \pm 0.10$ ($\nu = 0.15 \pm 0.08$)

for both ψ and Υ, as shown in Figs. 14 and 15. This behavior again corresponds to an effective potential which is a small positive power. It was this observation for the ψ family that led Machacek and Tomozawa [30] to investigate softer-than-linear confining potentials, including logarithmic forms. Taken together, these results on principal quantum number dependence would seem to exclude the bizarre possibility that the nearly equal spacing in the ψ and Υ families results from a potential strength which varies approximately as

$$\lambda \propto \mu^{\nu/2}. \tag{8.7}$$

Martin [29] has shown that careful attention to hyperfine effects does not change the conclusions of this analysis, namely that the interquark potential is flavor-independent (as QCD would have it) and characterized by an effective power-law potential with a small positive exponent. This is also in agreement with the conclusions of all other analyses and fits: In the region of space between 0.1 fm and 1 fm, the interaction between heavy quarks is flavor-independent, and roughly logarithmic in shape [31, 32].

9. Theorems and near theorems

An excellent review of statements about bound-state properties which may be proved rigorously in nonrelativistic potential theory has been given by Grosse and Martin [33]. Many results have been deduced which pertain to the order of levels, inequalities for wavefunctions at the origin, bounds on quark mass differences and so forth. The value of such statements is not only that they are true, but also that they provide a context for computations based upon explicit potentials. It is of great value to understand what must be true for any reasonable potential, or for any potential of a particular class, in order to distinguish the consequences that may be peculiar to a specific model. I shall cite two examples that bear directly upon experimental results.

Consider a quarkonium potential which is monotonic,

$$dV/dr \geqslant 0 \tag{9.1}$$

and concave downward,

$$d^2V/dr^2 \leqslant 0. \tag{9.2}$$

The first property is motivated by simplicity, and the second by the expectation that the confining potential rises no faster than linearly. Both are satisfied by the effective power-law potentials just discussed. Then if $m > \mu$ are masses of the constituents of two $Q\bar{Q}$ systems, one may prove [34] that

$$|\Psi_m(0)|^2 \geqslant (m/\mu)\,|\Psi_\mu(0)|^2. \tag{9.3}$$

This result holds for the ground state under the assumptions stated, for all levels in power-law potentials (compare Eq. (7.12)), and for all levels in a general potential satisfying the assumptions, in WKB approximation [33]. It implies a lower bound on leptonic widths in the more massive system as, in the case at hand,

$$\Gamma(\Upsilon_n \to e^+e^-) \geqslant \frac{m_b}{m_c} \cdot \frac{e_b^2}{e_c^2} \cdot \frac{M_{\psi_n}^2}{M_{\Upsilon_n}^2}\,\Gamma(\psi_n \to e^+e^-). \tag{9.4}$$

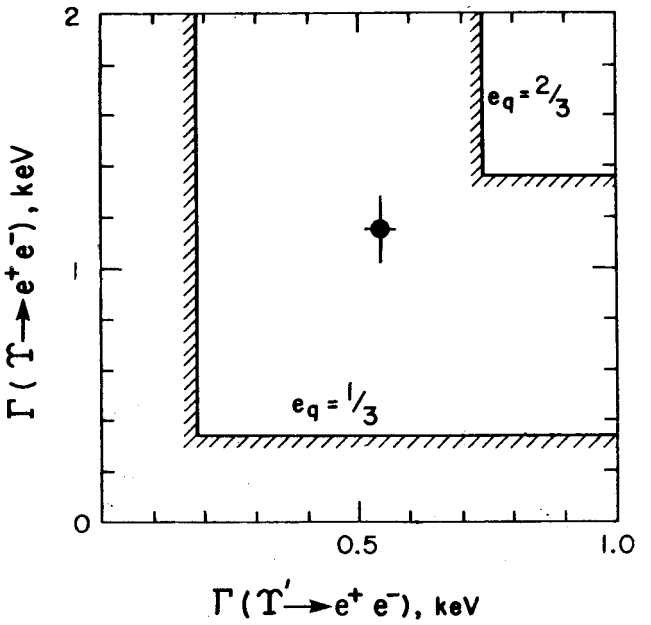

Fig. 16. Lower bounds for leptonic decays of Υ and Υ' (after Rosner, Quigg, and Thacker, Ref. [34]), together with the data cited in Table IV.The bounds are computed from Eq. (9.4) using ψ leptonic widths 1σ below the central values and assuming $m_b/m_c \geqslant 3$

The lower bounds on upsilon leptonic widths are plotted in Fig. 16, together with the experimental measurements. A b-quark charge of 2/3 is seen to be incompatible with the bound. The conclusion that $|e_b| = 1/3$ is substantiated by the measurements of $R = \sigma(e^+e^- \to \text{hadrons})/\sigma(e^+e^- \to \mu^+\mu^-)$.

By extrapolating from the upsilons to higher masses one may bound from below the integrated cross section for the production of the ground state of the next quarkonium family in e^+e^- annihilations[5]. Using cross section measurements from PETRA [35] it is possible to exclude on this basis a $t\bar{t}$ resonance (charge 2/3 quarks) below 38.63 GeV/c^2.

A semiclassical near-theorem relates the number of levels below flavor threshold to the mass of the constituents. This would seem to be a question ill-suited to a nonrelativistic approach because it is necessary to compute both quarkonium ($Q\bar{Q}$) masses and the mass of the lightest flavored ($Q\bar{q}$) state. The latter is unlikely to be governed by a potential theory description. However, a key simplifying observation was made by Eichten and Gottfried [36] who noted that the mass of the light quark-heavy quark state can be written as

$$M(Q\bar{q}) = M(Q) + M(q) + \text{binding} + \text{hyperfine}. \tag{9.5}$$

Although the binding energy may not be calculable, it is reasonable to suppose that it depends upon the reduced mass of the constituents, which tends to $M(q)$ as $M(Q) \to \infty$.

[5] See, for example, Fig. 10 of Quigg, Ref. [28].

Thus the binding energy must become independent of the heavy quark mass. Furthermore, the hyperfine splitting of the 0^{-+} and 1^{--} $(Q\bar{q})$ levels must certainly vary as $1/M(Q)$. It therefore vanishes as $M(Q) \to \infty$. Hence in the limit of infinite quark mass, the difference

$$\delta(M(Q)) \equiv 2M(Q\bar{q}) - 2M(Q) \to \delta_\infty, \tag{9.6}$$

independent of the heavy-quark mass.

In the regime in which $\delta(M(Q)) = \delta_\infty$ is a good approximation, the number of levels below flavor threshold is easily calculated [37]. Consider any confining potential. In semiclassical approximation the number of levels bound below $E = 2M(Q) + \delta_\infty$ is specified by the quantization condition

$$\int_0^{r_\delta} dr[M(Q)(\delta_\infty - V(r))]^{1/2} = (n - \tfrac{1}{4})\pi, \tag{9.7}$$

where to save writing the zero of energy has been set at $2M(Q)$. The classical turning point r_δ, defined through

$$V(r_\delta) = \delta_\infty \tag{9.8}$$

is independent of $M(Q)$, so we have by inspection the result that

$$(n - \tfrac{1}{4}) \propto \sqrt{M(Q)}. \tag{9.9}$$

It is likely that the limit (9.6) is already approached within 10% in the charmonium system, in which two $^3S_1$ levels lie below charm threshold. Thus there should be slightly less than four bound levels in the upsilon family, in agreement with the observation of three narrow vector states. The success of this prediction provides another verification of flavor independence, which was the principal assumption. Many narrow levels are thus to be expected for the next quarkonium family, when it is found, since the next quark mass certainly exceeds 18 GeV/c^2.

It is interesting to see how the result (9.9) is realized in specific potentials. To make this plain, I show in Fig. 17 the evolution with constituent mass of the spectra of the potentials $V(r) = -r^{-1/2}$, $V(r) = \ln r$ and $V(r) = r$, for which $\Delta E \sim \mu^{1/3}$, μ^0, and $\mu^{-1/3}$, respectively, according to (7.13). All the levels fall deeper into the wells as μ is increased. For the potential $V(r) = -r^{1/2}$, singular at the origin, the levels spread apart as they sink into the well. For the linear potential, no such pit exists, but the levels are packed more densely as μ increases. The logarithmic potential represents an intermediate case in which the level spacing is independent of the mass and levels drop into the well at a common rate given by

$$E_i(\mu') = E_i(\mu) - \tfrac{1}{2} \ln(\mu'/\mu). \tag{9.10}$$

In each case the rate of accumulation of levels below any specific value of the energy is given by (9.9).

A corollary to the conclusion that the classical turning point of the last narrow level

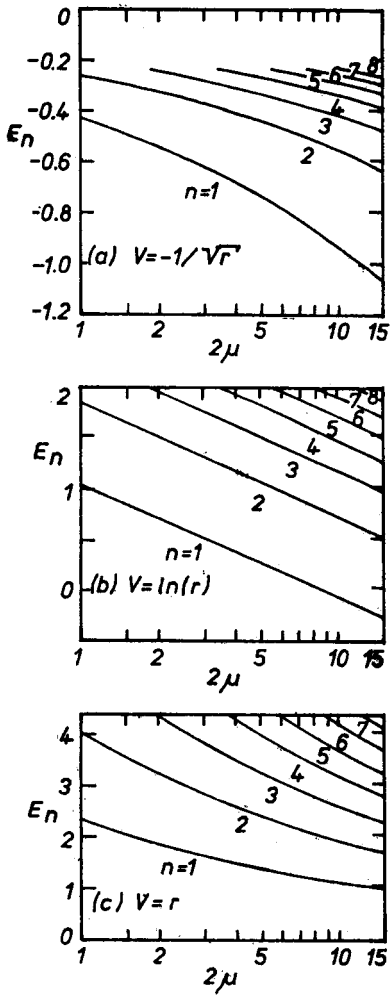

Fig. 17. Comparison of mass dependence of energy levels in three potentials: (a) $V(r) = -r^{-1/2}$; (b) $V(r) = \ln r$; (c) $V(r) = r$. (From Ref. [24])

has become independent of quark mass is that the single-channel analysis cannot be extended past about 1 fm. Heavier $(Q\bar{Q})$ systems will extend our knowledge of the interaction to shorter distances, but are unlikely to address the nature of the confining potential.

10. The inverse bound-state problem for quarkonium

In the preceding lecture we reviewed some of the motivation for an interest in heavy-quark spectroscopy, and investigated a few of the ways in which elementary methods of quantum mechanics can be useful. In this lecture we shall approach similar issues using different techniques. We seek answers to the following questions:

— How, and to what extent, does the spectrum of a quarkonium system measure the interquark potential?
— Where do we know the potential, and what is its form? The elementary analyses suggested that a form

$$V(r) = (730\ \text{MeV}) \log (r) \tag{10.1}$$

is a convenient summary for the ψ and Υ states.
— What information do we need to know the potential better?
— What conclusions may we draw about the force between quarks?

In addition, it is of interest to generate some expectations for the properties of the next quarkonium family, the $(t\bar{t})$ bound states. Our tool in this lecture will be the inverse scattering formalism.

We are all familiar with the direct problem of scattering theory, which consists in calculating the S-matrix from the equation of motion and the interaction. In typical non-relativistic applications the quantities to be computed are the bound-state positions and wavefunctions and the scattering amplitudes or phase shifts.

The inverse problem of scattering theory is complementary: given the equation of motion and the S-matrix, deduce the interaction. This is not the place for a thorough treatment of the inverse scattering problem, which has an immense literature, nor even to give a complete derivation of the results we shall use. Instead, we shall present some examples to make plausible the utility of the inverse formalism. We shall next pass on to a statement of the quantum mechanical problem first for finite potentials and then for confining potentials. There follows a review of the methodology followed in applications to quarkonium, and a study of the associated phenomenology of the ψ and Υ families. The lecture concludes with a summary of what has been learned and an outlook on future prospects.

11. Some simple inverse problems

Two examples will illustrate the sort of information (and assumptions!) required to determine a potential.

11.1. The classical inverse problem

In classical mechanics, knowledge of the period of oscillation as a function of energy is sufficient to determine uniquely a symmetric, monotonic potential. Consider a one-dimensional potential well of the kind shown in Fig. 18. The energy of a particle moving in such a well is given by

$$E = \frac{m\dot{x}^2}{2} + V(x). \tag{11.1}$$

Solving for

$$\dot{x} = \left(\frac{2(E-V)}{m}\right)^{1/2} \tag{11.2}$$

gives an expression for dt/dx which may be integrated to give the period

$$T(E) = 4\left(\frac{m}{2}\right)^{1/2} \int_0^{x(E)} \frac{dx}{\sqrt{E-V}}$$

$$= 2(2m)^{1/2} \int_0^{E} \frac{dV(dx/dV)}{\sqrt{E-V}}. \tag{11.3}$$

If we divide this equation by $\sqrt{\alpha-E}$, where α is for the moment a parameter satisfying

$$0 \leqslant V \leqslant E \leqslant \alpha, \tag{11.4}$$

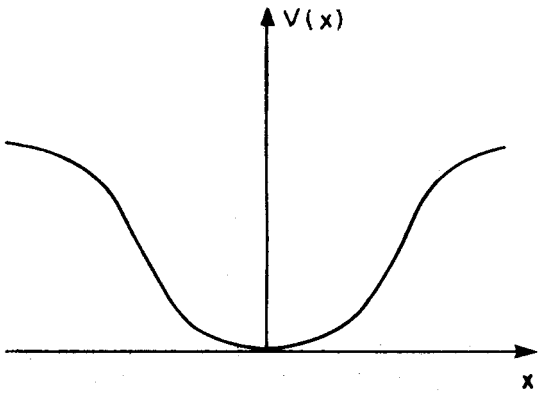

Fig. 18. A symmetric, monotonic potential in one dimension

integrate over the energy $\int_0^{\alpha} dE$, and interchange the order of integration, we find

$$\int_0^{\alpha} \frac{dET(E)}{\sqrt{\alpha-E}} = 2(2m)^{1/2} \int_0^{\alpha} dV(dx/dV) \int_V^{\alpha} \underbrace{dE[(E-V)(\alpha-E)]^{-1/2}}_{\pi}$$

$$= 2\pi(2m)^{1/2} x(\alpha). \tag{11.5}$$

Now replacing $\alpha \to V$, we obtain an expression for the shape of the potential in terms of the period,

$$x(V) = \frac{1}{2\pi(2m)^{1/2}} \int_0^{V} \frac{dET(E)}{\sqrt{V-E}}. \tag{11.6}$$

If, for example, the period is independent of energy, we readily find that

$$x(V) \propto \sqrt{V}, \tag{11.7}$$

or, in other words,

$$V(x) \propto x^2. \tag{11.8}$$

This is a familiar result.

11.2. The semiclassical inverse problem

Very similar arithmetic leads to the reconstruction, in semiclassical approximation, of a symmetric, monotonic potential in one dimension. In this instance we begin with the quantization condition

$$2\int_0^{x_0} dx[2\mu(E_n - V(x))]^{1/2} = (n+\tfrac{1}{2})\pi. \tag{11.9}$$

Differentiating both sides with respect to the principal quantum number n, we have

$$(2\mu)^{1/2}\int_0^x \frac{dx(\partial E/\partial n)}{\sqrt{E-V}} = \pi, \tag{11.10}$$

which may be rewritten as

$$\int_{V(0)\equiv 0}^{E} dV(dx/dV)\left[\frac{2\mu}{E-V}\right]^{1/2} = \frac{\pi}{\partial E/\partial n}. \tag{11.11}$$

This is quite similar in form to Eq. (11.3), and so we follow the same steps as before. Operating on the equation with $\int_0^\alpha dE(\alpha-E)^{-1/2}$ and interchanging the order of integration, we find

$$\int_0^\alpha dV(dx/dV)\int_V^\alpha \frac{dE}{(\alpha-E)^{1/2}(E-V)^{1/2}} = \pi\int_0^\alpha \frac{dE}{[2\mu(\alpha-E)]^{1/2}(\partial E/\partial n)}. \tag{11.12}$$

The $\int dE$ on the left-hand side is a Beta function whose value is π. Consequently upon renaming $\alpha \to V$ we are left with the result

$$x(V) = \int_0^V \frac{dE}{[2\mu(V-E)]^{1/2}(\partial E/\partial n)}. \tag{11.13}$$

Again it is worthwhile to examine an elementary case. Consider a constant level density

$$\partial E/\partial n = 2, \tag{11.14}$$

with mass

$$2\mu = 1. \tag{11.15}$$

An elementary computation gives the well-known result

$$x = \sqrt{V}, \tag{11.16}$$

or

$$V = x^2. \tag{11.17}$$

With these two examples to provide plausibility, we now turn to the general case in one-dimensional quantum mechanics.

12. The quantum-mechanical inverse problem

The general inverse problem in one-dimensional quantum mechanics as governed by the Schrödinger equation is highly developed. A finite potential which binds N bound states is completely specified by $2N$ bound-state parameters plus knowledge of the phase shift everywhere in the continuum[6]. The procedure, roughly speaking, is to write a dispersion relation for the Schrödinger wavefunction, for which one must specify the position and wavefunction normalization of each bound state (as poles and residues) and the reflection coefficient in the continuum (as a dispersion integral). Having such a representation of the wavefunction $\psi(x)$ and knowing the (Schrödinger) equation of motion, one may solve for the potential $V(x)$.

An interesting special case is that of a symmetric potential, for which the required bound-state information is reduced to N parameters — one for each bound state. A further simplification is obtained in the case of a symmetric potential which is also reflectionless, which is to say that an incident wave is completely transmitted, throughout the continuum. The simplest such potential is

$$V(x) = \frac{-2\kappa^2}{\cosh^2 \kappa x}. \tag{12.1}$$

For a particle of reduced mass ($2\mu = 1$) it binds a single level at

$$E_1 = -\kappa^2 \tag{12.2}$$

and has a vanishing reflection coefficient everywhere in the continuum. For potentials of this class, the dispersion integral disappears, and we are left with an N-parameter algebraic equation for a potential which binds N levels. Consequently, a symmetric, reflectionless potential is completely specified by the set of binding energies of its levels. The inverse Schrödinger problem for reflectionless potentials has a deep and interesting connection with soliton solutions to the Korteweg-de Vries equation [39].

The extensive development of the inverse scattering formalism has been concentrated on finite potentials, i.e., those which bind a finite number of levels. What can be done for a confining potential? It is natural [40] to try to build up a confining potential by a sequence of reflectionless approximations. A reflectionless approximant $V_N(x)$ is constructed to

[6] A partial bibliography is given in Ref. [38].

reproduce the first N levels of the true potential $V(x)$, and one hopes that in the limit of a large number of bound states,

$$\lim_{N\to\infty} V_N(x) \to V(x) \tag{12.3}$$

in some suitable sense.

It is intuitively reasonable that this procedure should provide a faithful representation of the true potential. This expectation is supported by a number of numerical examples, some of which are shown in Figs. 19–21. In the case of confining potentials, we must supplement the bound-state information with a choice of the ionization point $V_N(\pm\infty)$ for each approximant. We have found (through numerical experiments as well as analytic studies) that the choice

$$V_N(\pm\infty) = \tfrac{1}{2}(E_N + E_{N+1}) \tag{12.4}$$

yields sensible approximations. It satisfies the obvious requirements

$$E_N \leqslant V_N(\pm\infty) \leqslant E_{N+1}, \tag{12.5}$$

and has the advantage of being easy to remember. In the limit as $N \to \infty$, the details of this choice become unimportant.

Take first the case of the harmonic oscillator potential

$$V(x) = x^2, \tag{12.6}$$

which supports bound states at energies

$$E_n = 2n+1, \quad n = 0, 1, 2, \ldots \tag{12.7}$$

The first five reflectionless approximations to (12.6), with $V_N(\pm\infty)$ given by (12.4), are compared with the true potential in Fig. 19(a)–(e). The agreement is excellent in the region of x relevant to the specified energy levels. Successive approximations to the bound-state wave functions are plotted in Fig. 19(f)–(j). They are seen to converge rapidly toward the exact solutions shown in Fig. 19(k).

As a second example, consider the linear potential

$$V(x) = |x|, \tag{12.8}$$

for which the bound-state energies are given by the zeros of Airy functions

$$\begin{aligned} Ai'(-E_n) &= 0, \quad n = 1, 3, 5\ldots \\ Ai(-E_n) &= 0, \quad n = 2, 4, 6, \ldots \end{aligned} \tag{12.9}$$

This energy spectrum gives rise to the approximate potentials and wavefunctions displayed in Fig. 20. The agreement is again extremely encouraging.

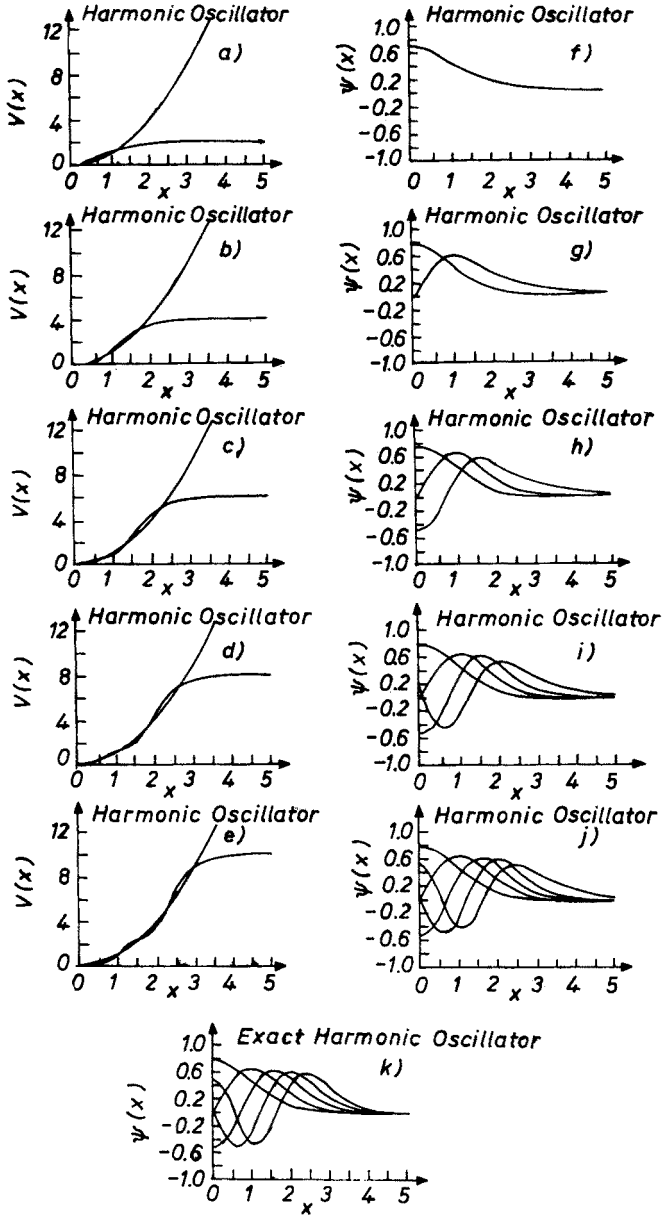

Fig. 19. Approximate reconstruction of the harmonic oscillator potential (a)–(e): $N = 1, 2, 3, 4, 5$ reflectionless approximations to the potential. The true potential is shown for comparison. (f)–(j): wave functions obtained in the $N = 1, 2, 3, 4, 5$ reflectionless approximations; (k) exact wave functions. (From Ref. [40])

Finally, it is well to examine the pathological case of an infinitely deep square-well potential

$$V(x) = \begin{cases} 0, & |x| < \pi/2 \\ \infty, & |x| > \pi/2 \end{cases} \tag{12.10}$$

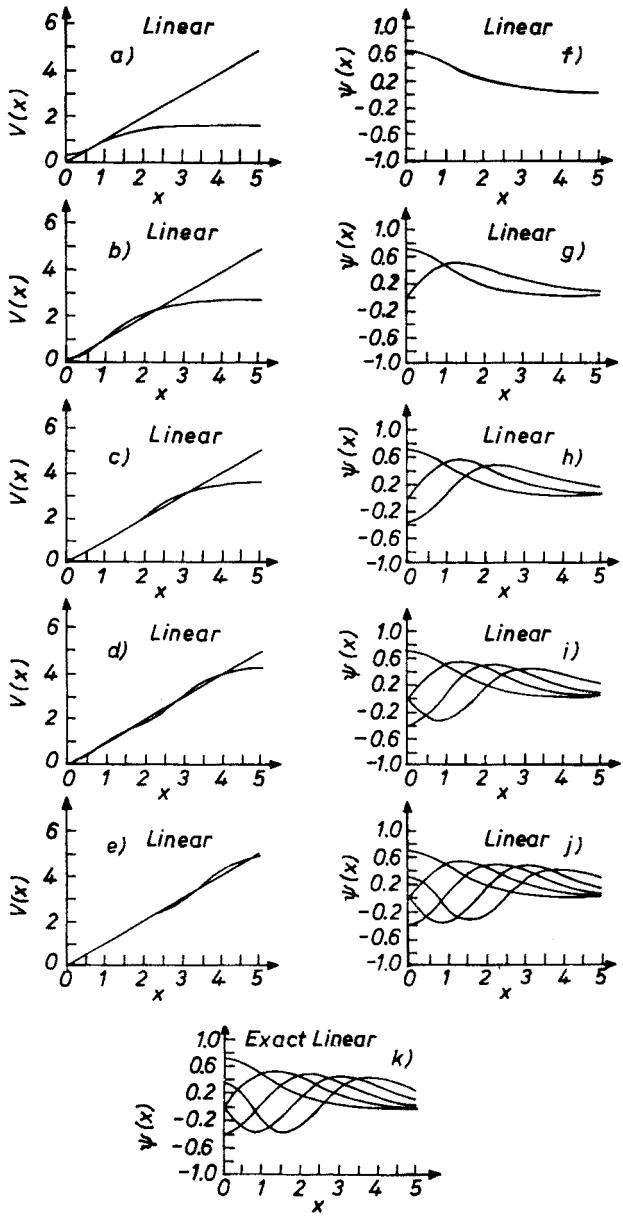

Fig. 20. Approximate reconstruction of the linear potential. See the caption to Fig. 19. (From Ref. [40])

which has bound states at

$$E_n = n^2, \quad n = 1, 2, \ldots \tag{12.11}$$

The reconstructed potentials are shown in Fig. 21(a)–(e). The agreement between exact and approximate forms is rather less striking than for the two preceding examples. The

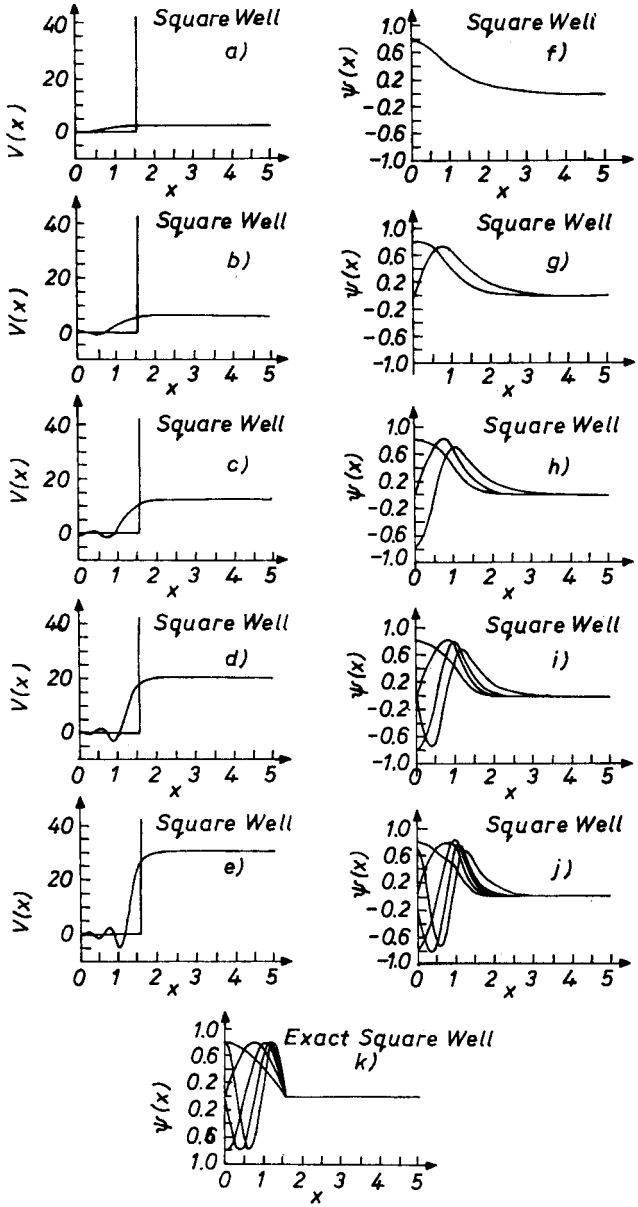

Fig. 21. Approximate reconstruction of the infinite square-well potential. See the caption to Fig. 19. (From Ref. [40])

manner in which the approximate wavefunctions plotted in Fig. 21(f)–(j) are increasingly excluded from the forbidden region of space is noteworthy, however.

These examples, which suggest the convergence of reflectionless approximations to nonpathological potentials, also indicate an acceptable rate of convergence. It has been possible to prove a number of limited statements about the fact of convergence [41–43], but nothing is known about the *rate* of convergence beyond what is indicated by the numerical experiments. In the numerical experiments reported here the potentials have been reconstructed from the binding energies of the levels of both odd and even parity. Alternatively, one may base the reconstruction on the states of either parity, in which case the binding energies must be supplemented with wave function information such as the value or slope of the wave function at the origin. Some of the proofs of convergence have been carried through for all three sets of input information.

13. Determinations of the quarkonium potential

In a series of publications [44–46], Rosner, Thacker, and I have extended the inverse scattering formalism for reflectionless potentials to the reconstruction of central potentials in three space dimensions, and have derived approximate interquark potentials from the quarkonium data. In this Section I will briefly summarize what we have done and what we think we have learned about the force between quarks.

The reduced radial Schrödinger equation for s-waves,

$$\frac{1}{2\mu} u''(r) + [E - V(r)]u(r) = 0, \tag{13.1}$$

is identical in form to the one-dimensional Schrödinger equation. As a consequence, the one-dimensional inverse scattering formalism can be applied to the study of quarkonium systems. However, because of the boundary condition

$$u(0) = 0 \tag{13.2}$$

imposed by the finiteness of the radial wave function at the origin, only the odd-parity levels in one dimension correspond to physical states. Therefore, in order to apply our one-dimensional formalism to the psions, we must regard the ψ and ψ' as the second and fourth levels of a symmetric one-dimensional potential $V(r) = V(-r)$. The even-parity levels which appear in the one-dimensional problem are interleaved with the physical psions, one below the ψ, one between the ψ and ψ', and so on.

To substitute in the reconstruction algorithm for the fictitious levels we require information about the slopes of the odd-parity reduced radial wavefunctions, or equivalently, the values of the three-dimensional wavefunctions at the origin. These are related in principle to the measured leptonic decay widths through the connection

$$|\Psi_n(0)|^2 = (1/16\pi\alpha^2 e_Q^2) \cdot \varrho \cdot M_n^2 \Gamma(V_n \to e^+ e^-). \tag{13.3}$$

With the parameter $\varrho = 1$, this is simply the Van Royen-Weisskopf formula [25] of nonrelativistic potential scattering. In a purely Coulombic quarkonium system, quantum

chromodynamics yields a correction

$$\varrho = \left[1 - \frac{16\alpha_s}{\pi} + O(\beta^2)\right]^{-1}, \tag{13.4}$$

where α_s is the strong coupling constant and β is the speed of the bound quark. Although the known quarkonium families are decidedly non-Coulombic, the belief that the strong coupling constant may be as large as $\alpha_s = 0.2$–0.3 has led many authors to suspect that ϱ may be appreciably greater than one.

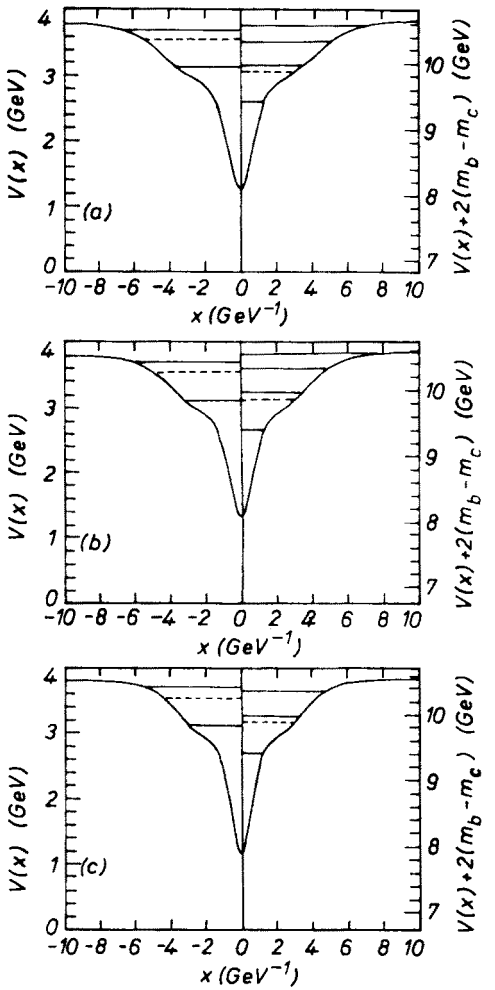

Fig. 22. Potentials constructed from the ψ and ψ'. (a) $\varrho = 1$, $m_c = 1.1\ \mathrm{GeV}/c^2$; (b) $\varrho = 1.4$, $m_c = 1.4\ \mathrm{GeV}/c^2$; (c) $\varrho = 2$, $m_c = 1.7\ \mathrm{GeV}/c^2$. Levels of the charmonium (Υ) system are plotted on the left (right). Solid lines denote the $^3S_1$ states; dashed lines indicate the mean mass of the 2^3P_J states. The right-hand scale (for the Υ's) is shifted by an amount $2(m_b - m_c)$ with respect to the left-hand (psion) scale. (From Ref. [46])

In the most recent analysis [46], we use as inputs to the charmonium potential the masses and leptonic widths of ψ and ψ', and choose the "ionization point" as[7]

$$E_0 = V(\pm\infty) = 3.8 \text{ GeV}. \tag{13.5}$$

This is halfway between the ψ' and the first omitted fictitious (even-parity) level, estimated by

$$E_0 = \frac{3M(\psi') + M(4.028)}{4}. \tag{13.6}$$

To explore the effects of our ignorance of strong radiative corrections to the decay rate, we take as representative values of the multiplicative correction to the van Royen-Weisskopf

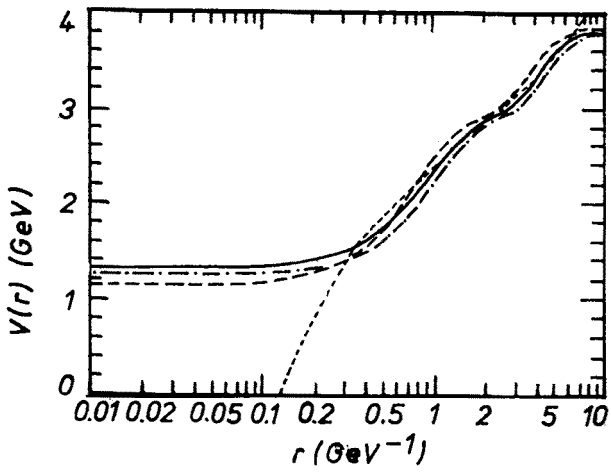

Fig. 23. Comparison of the charmonium potentials of Fig. 22. Dot-dashed line: $\varrho = 1$, $m_c = 1.1$ GeV/c^2; solid line: $\varrho = 1.4$, $m_c = 1.4$ GeV/c^2; long-dashed line: $\varrho = 2$, $m_c = 1.7$ GeV/c^2. The short-dashed line is the "asymptotic freedom" potential of Ref. [31]. (From Ref. [46])

formula $\varrho = 1$ (which corresponds to no correction), and $\varrho = 1.4$ and 2. We believe, but cannot prove, that $\varrho = 2$ represents a larger correction than is plausible, and intend that the extremes $\varrho = (1, 2)$ bracket the true value.

Although only s-wave information is used systematically in the inverse-scattering algorithm, information about other partial waves may be used to discriminate among potentials constructed under varying assumptions for the quark mass. For each value of ϱ, we select the value of the charmed quark mass m_c which correctly reproduces the center of gravity of the 2^3P_J χ states. The resulting potentials are shown in Fig. 22. For each potential we choose a value of the b-quark mass which reproduces the mass of the Υ ground state, and then compute the complete upsilon spectrum. The agreement with experiment is quite satisfying.

The three charmonium potentials are compared in Fig. 23. In the range $0.5 \text{ GeV}^{-1} \leqslant r \leqslant 5 \text{ GeV}^{-1}$, the potentials vary approximately logarithmically with the interquark

[7] The CESR energy scale was adopted for this analysis. Energies should be increased by about 25 MeV.

separation, as expected on the basis of the scaling arguments reviewed in the first lecture. The local fluctuations are artifacts of the reflectionless approximant technique. Also shown in Fig. 23 (as the short-dashed line) is the shape of the QCD-inspired potential of Buchmüller and Tye [31], which is typical of explicit potentials that provide a good representation of ψ and Υ data. In the region of space to which charmonium observables are sensitive, it provides a smooth interpolation of the inverse-scattering results.

The method of constructing potentials from the upsilon family differs only slightly in detail. In this case we took as inputs the masses and leptonic widths of the $1S-4S$

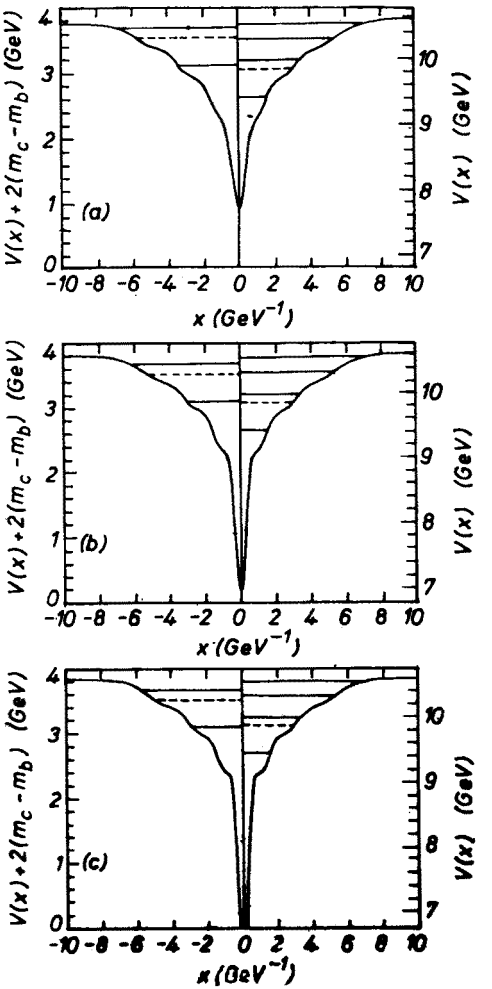

Fig. 24. Potentials reconstructed from the Υ spectrum (a) $\varrho = 1$, $m_b = 4.5\ \mathrm{GeV}/c^2$; (b) $\varrho = 1.4$, $m_b = 4.75\ \mathrm{GeV}/c^2$; (c) $\varrho = 2$, $m_b = 5\ \mathrm{GeV}/c^2$. Levels of the upsilon (charmonium) system are plotted on the right (left). Solid lines denote the $^3S_1$ states; dashed lines indicate the mean mass of the 2^3P_J states. The left-hand scale (for the psions) is shifted by an amount $2(m_c - m_b)$ with respect to the right-hand (upsilon) scale. (From Ref. [46])

levels, and chose as ionization point the value

$$E_0 = \frac{5M(4S) - M(3S)}{4} = 10.6 \text{ GeV}. \tag{13.7}$$

Since the spectrum of p-wave states is not yet well established, we were not able to use the P-states to select the "best" value of the b-quark mass[8]. We therefore chose m_b for each ϱ rather arbitrarily to be close to the value needed to reproduce the $\Upsilon(1S)$ mass in the corresponding charmonium potential. Although this does not lead to appreciable ambiguity in our conclusions, it represents an indefiniteness that one would hope eventually to overcome. The resulting potentials are shown in Fig. 24. For each of them we choose a value of the charmed quark mass m_c which reproduces the mass of the ψ ground state. Again, the agreement between prediction and observation is satisfactory.

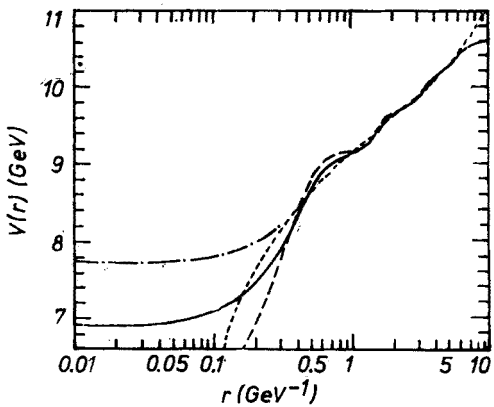

Fig. 25. Comparison of the upsilon potentials of Fig. 24. Dot-dashed line: $\varrho = 1$, $m_b = 4.5$ GeV/c^2; solid line: $\varrho = 1.4$, $m_b = 4.75$ GeV/c^2; long-dashed line: $\varrho = 2$, $m_b = 5$ GeV/c^2. The short-dashed line is the "asymptotic freedom" potential of Ref. [31]. (From Ref. [46])

The three Υ potentials are compared in Fig. 25. They are essentially indistinguishable for interquark separations larger than 0.4 GeV^{-1}. They also approximately coincide with other potentials that reproduce the data. Like the charmonium potentials of Fig. 23, the Υ potentials behave approximately logarithmically in the interval 0.5 GeV$^{-1} \leqslant r \leqslant 5$ GeV^{-1}. At distances smaller than 0.4 GeV^{-1} there is considerable variation among the potentials. This provides a measure of our current ignorance of the interaction between quarks at short distances.

The potentials constructed from the ψ and Υ families are compared with one another for equal values of the parameter ϱ in Fig. 26, where they have been superposed by requiring that the $\psi(3097)$ levels coincide. The agreement in each case is excellent for $r \geqslant 0.5$ GeV^{-1} (0.1 fm), where both quarkonium systems provide information. The comparison provides

[8] Our expectations for the $3P(b\bar{b})$ center of gravity are in reasonable accord with the measurement reported in Sec. 6.

direct evidence that the strong (quark-antiquark) interaction is flavor-independent in the range 0.1 fm $< r <$ 1 fm. This conclusion is supported by the quantitative agreement of predictions from ψ potentials with Υ observables and of predictions from Υ potentials with ψ observables.

A number of refinements to this analysis can be envisaged. Knowledge of the positions of the 2^3P_J, 3^3P_J, and 4^3P_J levels in the upsilon family and improved measurements of the leptonic widths of all the $^3S_1$ quarkonium levels will make possible more precise determinations of the potential. Detailed studies of the $E1$ transition rates for the upsilon will test in a different manner the nonrelativistic picture of quarkonium. The fine structure of the

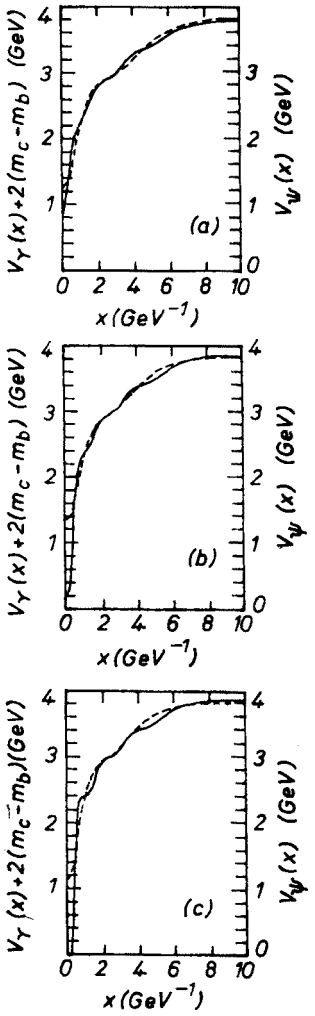

Fig. 26. Comparison of potentials deduced from the ψ and Υ families. The energy scale is appropriate for the ψ spectrum. In each graph, the label on the left-hand ordinate refers to the potential constructed using Υ data (solid curve). The label on the right-hand ordinate refers to the potential constructed using psion data (dashed curve). (a) $\varrho = 1$; (b) $\varrho = 1.4$; (c) $\varrho = 2$. (From Ref. [46])

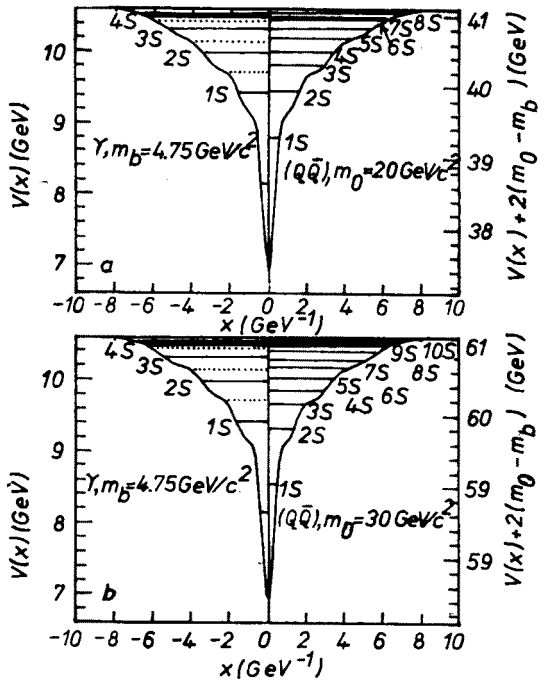

Fig. 27. Relative positions of Υ and (QQ̄) levels in the $\varrho = 1.4$, $m_b = 4.75$ GeV/c^2 potential. The $^3S_1$ levels are indicated by solid lines. The fictitious "even-parity" levels of the Υ problem are shown as dotted lines. Shaded bands denote the flavor threshold (a) $m_Q = 20$ GeV/c^2; (b) $m_Q = 30$ GeV/c^2. (From Ref. [47])

^3P states and locations of the ^1P states hold important clues to the Lorentz structure of the interquark interaction. An extension of our "measurements" of the potential to larger distances is unlikely because the single-channel description is inappropriate above flavor threshold. As we saw in Section 9, it is plausible that the dissociation radius is flavor-independent and approximately equal to 1 fm. To extend our knowledge to shorter distances we require a more massive quarkonium family. By virtue of the general result (9.9), the next quarkonium family will contain eight or more narrow $^3S_1$ levels, which would both extend and refine our knowledge of the potential. Some projections based upon the upsilon system are shown in Fig. 27.

14. Outlook

The ψ and Υ quarkonium systems have made accessible to us a considerable amount of new information about the force between quarks. What has been learned ranges from the qualitative insight that nonrelativistic methods are apt to a rather precise determination of the interquark potential at distances between about 0.1 fm and 1 fm. Some of the analysis techniques which lead to a determination of the potential have been reviewed in these lectures. There are other important issues that we have not touched on here in Zakopane. Among them are the general problem of fine structure and the spacetime form of the

interaction, and the quantitative application of perturbative QCD to quarkonium decay rates. Both of these seem ripe for significant development. In all areas we would benefit enormously from the observation and detailed study of one more quarkonium family below the mass of the Z^0.

REFERENCES

[1] K. G. Wilson, *Phys. Rev.* **D10**, 2445 (1974); M. Creutz, *Phys. Rev. Lett.* **43**, 553 (1979).

[2] C. Quigg, *Models for Hadrons*, FERMILAB-Conf-81/78-THY to appear in *Gauge Theories in High Energy Physics*, edited by M. K. Gaillard and R. Stora, North-Holland, Amsterdam 1983, p. 645.

[3] H. Hamber, G. Parisi, *Phys. Rev. Lett.* **47**, 1792 (1981); E. Marinari, G. Parisi, C. Rebbi, *Phys. Rev. Lett.* **47**, 1795 (1981); D. H. Weingarten, *Phys. Lett.* **109B**, 57 (1982); A. Hasenfratz, Z. Kunst, P. Hasenfratz, C. B. Lang, *Phys. Lett.* **110B**, 289 (1982); C. Bernard, T. Draper, K. Olynyk, UCLA/82/TEP/22, December 1982.

[4] A. De Rujula, H. Georgi, S. L. Glashow, *Phys. Rev.* **D12**, 147 (1975).

[5] G. Karl, in Proceedings of the 19th International Conference on High Energy Physics, Tokyo 1978, edited by S. Homma, M. Kawaguchi, and H. Miyazawa, Physical Society of Japan, Tokyo 1979, p. 135; A. J. G. Hey, in Proceedings of the 1979 European Physical Society Conference on Particle Physics, CERN, Geneva, p. 523; and in *Baryon 1980*, IVth International Conference on Baryon Resonances, Toronto, edited by N. Isgur, University of Toronto, p. 223; N. Isgur, in *High Energy Physics-1980*, XXth International Conference, Madison, edited by L. Durand and L. G. Pondrom, American Institute of Physics, New York, p. 30; and in *New Aspects of Subnuclear Physics*, International School of Physics "Ettore Majorana", 1978, edited by A. Zichichi, Plenum, New York 1980; F. Close, Proc. European Physical Society Conference on High Energy Physics, Lisbon 1981, edited by J. Dias de Deus and J. Soffer, European Physical Society, 1983, p. 549.

[6] I. Cohen, H. J. Lipkin, *Nucl. Phys.* **B151**, 16 (1979).

[7] R. L. Jaffe, *Phys. Rev. Lett.* **38**, 195 (1977).

[8] A. S. Carroll et al., *Phys. Rev. Lett.* **41**, 777 (1978).

[9] R. L. Jaffe, K. Johnson, *Phys. Lett.* **60B**, 201 (1976); R. L. Jaffe, *Phys. Rev.* **D15**, 267 (1977); R. L. Jaffe, F. E. Low, *Phys. Rev.* **D19**, 2105 (1979); A. J. G. Hey, in *High-Energy Physics-1980*, XXth International Conference, Madison, edited by L. Durand and L. G. Pondrom, American Institute of Physics, New York, p. 22.

[10] L. Montanet, G. C. Rossi, G. Veneziano, *Phys. Rep.* **63C**, 149 (1980).

[11] F. Close, Ref. [5]; D. Horn, J. Mandula, *Phys. Rev.* **D17**, 898 (1978); K. C. Bowler, P. J. Corvi, A. J. G. Hey, P. D. Jarvis, *Phys. Rev. Lett.* **45**, 97 (1980); F. de Viron, J. Weyers, *Nucl. Phys.* **B185**, 391 (1981); M. Chanowitz, S. Sharpe, LBL-14865 (1982).

[12] R. C. Giles, S.-H. H. Tye, *Phys. Rev.* **D16**, 1079 (1977); *Phys. Lett.* **73B**, 30 (1978); W. Buchmüller, S.-H. H. Tye, *Phys. Rev. Lett.* **44**, 850 (1980).

[13] H. Fritzsch, M. Gell-Mann, in Proceedings of the XVI International Conference on High Energy Physics, edited by J. D. Jackson, A. Roberts, and R. Donaldson, Fermilab, Batavia 1972, p. II-135; J. D. Bjorken, in Proceedings of the European Physical Society Conference on High Energy Physics, CERN, Geneva 1979, p. 245; in *Quantum Chromodynamics*, Proceedings of the 7th SLAC Summer Institute on Particle Physics, SLAC, Stanford 1979, p. 219.

[14] C. Edwards et al., *Phys. Rev. Lett.* **49**, 259 (1982).

[15] C. Edwards et al., *Phys. Lett.* **110B**, 82 (1982).

[16] C. Edwards et al., *Phys. Rev.* **D25**, 3065 (1982).

[17] T. Appelquist, H. D. Politzer, *Phys. Rev. Lett.* **34**, 43 (1975).

[18] E. Eichten, K. Gottfried, T. Kinoshita, J. Kogut, K. D. Lane, T.-M. Yan, *Phys. Rev. Lett.* **34**, 369 (1975).

[19] J. Gaiser et al., SLAC-PUB-2899 (1982).

[20] C. Edwards et al., *Phys. Rev. Lett.* **48**, 70 (1982).
[21] A. S. Artamonov et al., *Phys. Lett.* **118B**, 225 (1982).
[22] K. Han et al., *Phys. Rev. Lett.* **49**, 1612 (1982); G. Eigen et al., *Phys. Rev. Lett.* **49**, 1616 (1982); J. Lee-Franzini, *What have we learned from the upsilons?*, invited talk at the SLAC Topical Conference, August 1982.
[23] S. Behrends et al., *Phys. Rev. Lett.* **50**, 881 (1983).
[24] C. Quigg, J. L. Rosner, *Phys. Rep.* **56C**, 167 (1979).
[25] R. Van Royen, V. F. Weisskopf, *Nuovo Cimento* **50**, 617 (1967); **51**, 583 (1967).
[26] C. Quigg, J. L. Rosner, *Phys. Lett.* **71B**, 153 (1977).
[27] C. Quigg, J. L. Rosner, *Comments Nucl. Part. Phys.* **8**, 11 (1978).
[28] C. Quigg, in Proceedings of the 1979 International Symposium on Lepton and Photon Interactions at High Energies, edited by T.B.W. Kirk and H.D.I. Abarbanel, Fermilab, Batavia 1980, p. 239; J. L. Rosner, in *Particles and Fields-1979*, edited by B. Margolis and D. G. Stairs, American Institute of Physics, New York, p. 325; in *Techniques and Concepts of High Energy Physics*, edited by T. Ferbel, Plenum, New York 1981, p. 1.
[29] A. Martin, *Phys. Lett.* **93B**, 338 (1980).
[30] M. Machacek, Y. Tomozawa, *Ann. Phys.* (NY) **110**, 407 (1978).
[31] W. Buchmüller, S.-H. H. Tye, *Phys. Rev.* **D24**, 132 (1981).
[32] C. Quigg, J. L. Rosner, *Phys. Rev.* **D23**, 2625 (1981).
[33] H. Grosse, A. Martin, *Phys. Rep.* **60C**, 341 (1980).
[34] J. L. Rosner, C. Quigg, H. B. Thacker, *Phys. Lett.* **74B**, 350 (1978); C. N. Leung, J. L. Rosner, *J. Math. Phys.* **20**, 1435 (1979).
[35] B. Adeva et al., *Phys. Rev. Lett.* **50**, 799 (1983).
[36] E. Eichten, K. Gottfried, *Phys. Lett.* **66B**, 286 (1977).
[37] C. Quigg, J. L. Rosner, *Phys. Lett.* **72B**, 462 (1978).
[38] I. M. Gel'fand, B. M. Levitan, *Am. Math. Soc. Trans.* **1**, 253 (1955); I. Kay, H. E. Moses, *J. Appl. Phys.* **27**, 1503 (1956).
[39] C. S. Gardner, J. M. Greene, M. D. Kruskal, R. M. Miura, *Phys. Rev. Lett.* **19**, 1095 (1967); *Comm. Pure Appl. Math.* **27**, 97 (1974).
[40] H. B. Thacker, C. Quigg, J. L. Rosner, *Phys. Rev.* **D18**, 274 (1978).
[41] H. Grosse, A. Martin, *Nucl. Phys.* **B148**, 413 (1979).
[42] J. F. Schonfeld et al., *Ann. Phys.* (NY) **128**, 1 (1980).
[43] I. Sabba Stefanescu, Karlsruhe preprint TKP-81-1.
[44] H. B. Thacker, C. Quigg, J. L. Rosner, *Phys. Rev.* **D18**, 287 (1978).
[45] C. Quigg, H. B. Thacker, J. L. Rosner, *Phys. Rev.* **D21**, 234 (1980).
[46] C. Quigg, J. L. Rosner, *Phys. Rev.* **D23**, 2625 (1981).
[47] P. Moxhay, J. L. Rosner, C. Quigg, *Phys. Rev.* **D23**, 2638 (1981).